AGU PUBLICATIONS

Geochemistry, Geophysics, Geosystems

RESEARCH ARTICLE
10.1002/2016GC006398

A distinct source and differentiation history for Kolumbo submarine volcano, Santorini volcanic field, Aegean arc

Martijn Klaver[1,2], Steven Carey[3], Paraskevi Nomikou[4], Ingrid Smet[5], Athanasios Godelitsas[4], and Pieter Vroon[1]

[1]Department of Geology and Geochemistry, Vrije Universiteit Amsterdam, Amsterdam, Netherlands, [2]Now at Bristol Isotope Group, School of Earth Sciences, University of Bristol, Bristol, UK, [3]Graduate School of Oceanography, University of Rhode Island, Kingston, Rhode Island, USA, [4]Faculty of Geology and Geo-Environment, National and Kapodistrian University of Athens, Athens, Greece, [5]Department of Geology, Ghent University, Ghent, Belgium

Key Points:
- A trace element and Sr-Nd-Hf-Pb isotope study of Kolumbo submarine volcano within the Santorini volcanic field
- The magmatic systems of Kolumbo and Santorini are unrelated and Kolumbo taps a distinct enriched mantle source
- Mantle source variations can be manifested in temporally associated arc magmas within the same volcanic field

Supporting Information:
- Supporting Information S1
- Data Set S1

Correspondence to:
M. Klaver,
martijn.klaver@bristol.ac.uk

Citation:
Klaver, M., S. Carey, P. Nomikou, I. Smet, A. Godelitsas, and P. Vroon (2016), A distinct source and differentiation history for Kolumbo submarine volcano, Santorini volcanic field, Aegean arc, *Geochem. Geophys. Geosyst.*, *17*, 3254–3273, doi:10.1002/2016GC006398.

Received 13 APR 2016
Accepted 5 JUL 2016
Accepted article online 11 JUL 2016
Published online 16 AUG 2016

© 2016. The Authors. Geochemistry, Geophysics, Geosystems published by Wiley Periodicals, Inc. on behalf of American Geophysical Union.

This is an open access article under the terms of the Creative Commons Attribution-NonCommercial-NoDerivs License, which permits use and distribution in any medium, provided the original work is properly cited, the use is non-commercial and no modifications or adaptations are made.

Abstract This study reports the first detailed geochemical characterization of Kolumbo submarine volcano in order to investigate the role of source heterogeneity in controlling geochemical variability within the Santorini volcanic field in the central Aegean arc. Kolumbo, situated 15 km to the northeast of Santorini, last erupted in 1650 AD and is thus closely associated with the Santorini volcanic system in space and time. Samples taken by remotely-operated vehicle that were analyzed for major element, trace element and Sr-Nd-Hf-Pb isotope composition include the 1650 AD and underlying K2 rhyolitic, enclave-bearing pumices that are nearly identical in composition (73 wt.% SiO_2, 4.2 wt.% K_2O). Lava bodies exposed in the crater and enclaves are basalts to andesites (52–60 wt.% SiO_2). Biotite and amphibole are common phenocryst phases, in contrast with the typically anhydrous mineral assemblages of Santorini. The strong geochemical signature of amphibole fractionation and the assimilation of lower crustal basement in the petrogenesis of the Kolumbo magmas indicates that Kolumbo and Santorini underwent different crustal differentiation histories and that their crustal magmatic systems are unrelated. Moreover, the Kolumbo samples are derived from a distinct, more enriched mantle source that is characterized by high Nb/Yb (>3) and low $^{206}Pb/^{204}Pb$ (<18.82) that has not been recognized in the Santorini volcanic products. The strong dissimilarity in both petrogenesis and inferred mantle sources between Kolumbo and Santorini suggests that pronounced source variations can be manifested in arc magmas that are closely associated in space and time within a single volcanic field.

1. Introduction

Kolumbo is a submarine volcano that is situated ca. 15 km to the northeast of the center of Santorini caldera in the central part of the Aegean arc, Greece [*Sigurdsson et al*., 2006; *Nomikou et al*., 2012, 2013b]. Between September and November 1650 AD, Kolumbo erupted violently, resulting in the death of livestock and over 60 inhabitants on Santorini due to the release of noxious gasses [*Fouqué*, 1879; *Dominey-Howes et al*., 2000; *Cantner et al*., 2014; *Nomikou et al*., 2014a]. Ash fallout reached as a far as mainland Turkey and a pumice edifice rose above sea level, but was quickly eroded to below the wave base. Today, the products of the 1650 AD eruption in the surviving submarine crater comprise a ca. 250 m thick sequence of white, crystal poor pumices of rhyolitic composition [*Cantner et al*., 2014] that overlay an older cone-shaped structure [*Nomikou et al*., 2012]. A recent multichannel reflection seismic study identified five distinct volcanic units, thus establishing that Kolumbo has a polygenetic, composite structure [*Hübscher et al*., 2015] (Figure 1). Two of these units, the K2 pumice and 1650 AD pumice (unit K5 in *Hübscher et al*. [2015]), and several poorly defined intrusive bodies are exposed in the crater walls. The cone-shaped 3D geometry of the Kolumbo deposits indicates that their source is the Kolumbo vent and that they do not represent distal deposits of the major Plinian eruptions of Santorini. Whether the magmatic systems of Kolumbo and Santorini are related at depth, however, is uncertain. A recent tomographical study has suggested that the shallow (5–7 km depth) magma chamber underneath Kolumbo has a possible lateral extension toward the plumbing system of Santorini [*Dimitriadis et al*., 2010]. A possible link between the two magmatic systems implies that the Kolumbo volcanic products could be genetically related to the recent Nea Kameni dacites on Santorini (197 BC to present [*Druitt et al*., 1999]). Alternatively, the silicic 1650 AD pumices could represent evolved residual

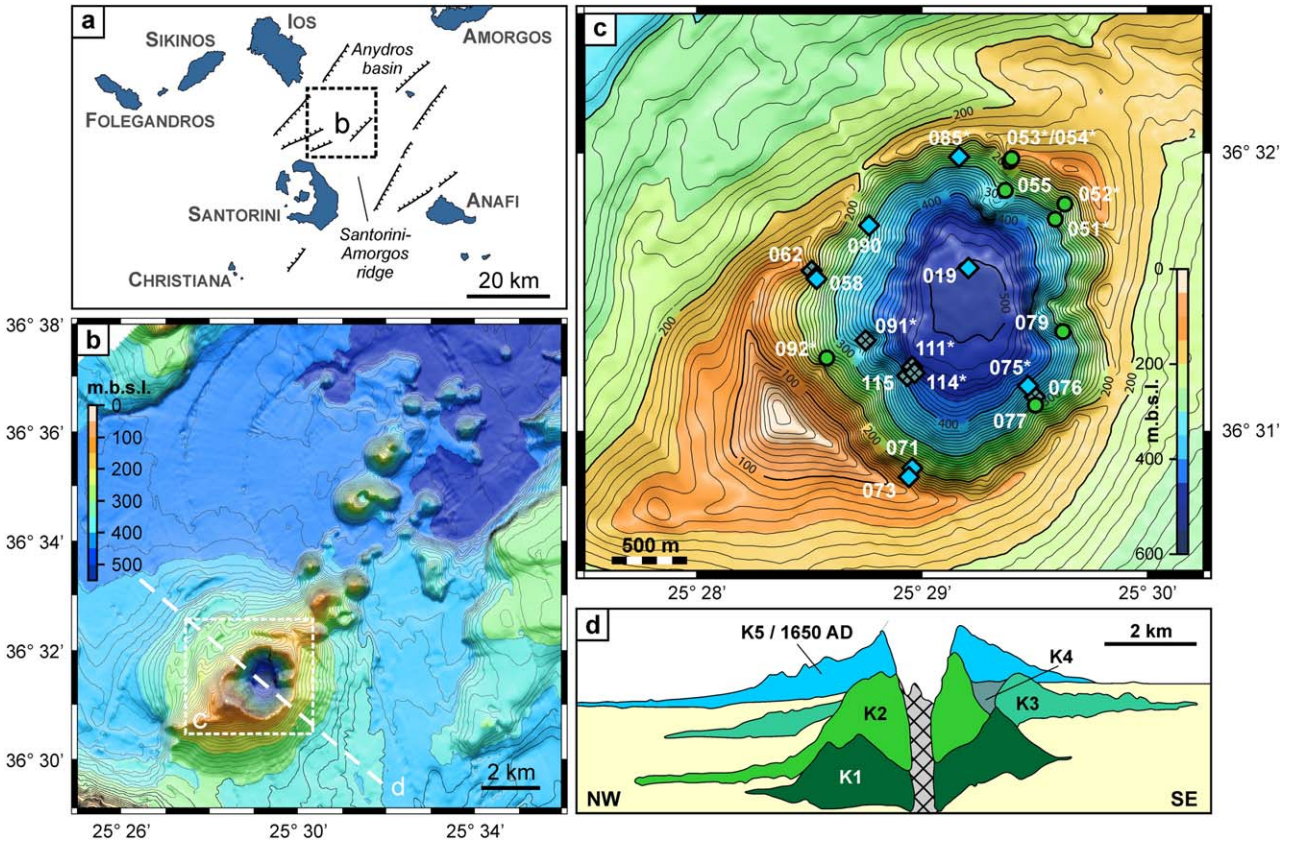

Figure 1. Location of the Kolumbo volcanic field and geometry of the Kolumbo crater. (a) Location map of the southern Cyclades islands, Greece. The Santorini volcanic field comprises Santorini, the Christiana islands and the submarine Kolumbo volcanic chain. The Christiana-Santorini-Kolumbo (CSK) tectonic line is formed by the extensional fault zone that links the Anydros basin and Santorini-Amorgos ridge. Location of faults adapted from *Dimitriadis et al*. [2010]; (b) Bathymetric map of the Kolumbo volcanic chain after *Nomikou et al*. [2012]; (c) Detailed bathymetric map of Kolumbo submarine volcano after *Nomikou* [2004]. Sampling locations are indicated and color coded for the different sample groups: blue diamonds – 1650 AD pumice, green circles – K2 pumice, sea green crossed diamonds – lavas. Samples with an * are grouped on the basis of major element composition rather than petrography and are not analyzed for trace element and Sr-Nd-Hf-Pb isotope composition; (d) Interpreted cross section of the Kolumbo cone along the transect shown in (b), modified after *Hübscher et al*. [2015]. Five distinct volcanic units have been recognized, of which only the K2 and 1650 AD pumice deposits are exposed in the crater walls (vertical exaggeration 7 times).

magma from the caldera-forming 3.6 ka Minoan eruption of Santorini, or the two volcanoes could be unrelated. The aim of this study is to establish if magmas of Kolumbo and Santorini follow the same crustal differentiation trends and therefore if their volcanic plumbing systems are related. The latter is of particular interest for the assessment of volcanic risks in the Santorini volcanic field. We have undertaken a comprehensive petrological and geochemical study of Kolumbo volcanic products that were sampled from the crater walls with the use of a remotely-operated vehicle (ROV) [*Carey et al*., 2011; *Bell et al*., 2012]. The first trace element and radiogenic isotope data are reported for Kolumbo submarine volcano, which include high-precision double spike Pb isotope analyses. These new data contribute toward the understanding of the dynamics of magma generation and differentiation in the central section of the Aegean arc.

2. Geological Setting

Kolumbo and 19 smaller (<2 km^2) submarine volcanic cones form a chain that constitutes the northernmost part of the Santorini volcanic field (Figure 1) [*Nomikou et al*., 2012, 2013a]. The Santorini volcanic field is one of the main volcanic centers of the Aegean arc, which has formed as a result of northward subduction of the African plate underneath Eurasia. Slab roll-back has induced active extension in the Aegean region and southward migration of the volcanic front, demonstrated by the onset of activity in the present Aegean arc at ca. 4 Ma [e.g., *Pe-Piper and Piper*, 2005]. The extensional tectonic regime in the southern Aegean strongly controls the locus of volcanism in the Santorini volcanic field. As a result, the Christiana Islands, Santorini and the Kolumbo volcanic chain have developed along the Christiana-Santorini-Kolumbo (CSK) tectonic line

(Figure 1) [*Nomikou et al*., 2013b] where active NW-SE extension facilitates the rise of magma. Recent strong seismic activity in the Kolumbo volcanic field [*Bohnhoff et al*., 2006; *Dimitriadis et al*., 2010] and the 2011–2012 unrest at Santorini have been attributed to magma movement underneath the Santorini volcanic field [e.g., *Newman et al*., 2012; *Parks et al*., 2012; *Feuillet*, 2013].

The present-day Kolumbo crater is roughly oval shaped with a diameter of ca. 1700 m and a depth of ca. 500 m b.s.l. to the crater floor with the highest point of the crater rim at 18 m b.s.l. (Figure 1) [*Nomikou*, 2004; *Nomikou et al*., 2012, 2013a]. Due to this geometry and the presence of an active hydrothermal field [*Sigurdsson et al*., 2006], a stagnant layer of dense, CO_2-rich water has accumulated inside the crater [*Carey et al*., 2013], which has facilitated the development of microbial activity and hydrothermal Tl-Sb-rich mineralization that are unique amongst hydrothermal systems worldwide [*Kilias et al*., 2013; *Oulas et al*., 2016]. At least five distinct volcanic units have been identified in Kolumbo on the basis of seismic imaging [*Hübscher et al*., 2015], as well as several poorly defined shallow intrusive bodies that have been interpreted as a set of NE-SW dykes [*Kilias et al*., 2013]. The youngest volcanic products of Kolumbo comprise an over 250 m thick package of stratified pumices that was deposited during the 1650 AD eruption and is described in detail by *Cantner et al*. [2014]. At present, there are no absolute geochronological constraints on the age of the underlying volcanic units, although *Hübscher et al*. [2015] correlate the K2 pumice with the 145 ka Middle Tuffs of Santorini [*Keller et al*., 2000] on the basis of the thickness of the intercalated sediments. This presumed age implies that volcanic activity of Kolumbo was synchronous with the second explosive cycle on Santorini [*Druitt et al*., 1999]. Of particular interest for investigating a relationship between Santorini and the 1650 AD eruption of Kolumbo are the most recent volcanic products of Santorini, the Minoan Tuff and the Kameni dacites. The rhyodacitic Minoan Tuff was emplaced during the last major, caldera-forming eruption of Santorini that marked the end of the second explosive cycle at 1627–1620 BC [*Friedrich et al*., 2006] and is described in detail in *Cottrell et al*. [1999] and *Druitt* [2014]. After the Minoan caldera collapse, subaerial activity resumed in 197 BC with the extrusion of dacitic lava flows on the island of Palaea Kameni in the center of Santorini caldera. On adjacent Nea Kameni, subaerial dacitic lavas have been emplaced intermittently from 1570 to 1950 AD [*Druitt et al*., 1999; *Martin et al*., 2006; *Nomikou et al*., 2014b] and hence these Kameni dacites have a close temporal association with the 1650 AD eruption of Kolumbo.

3. Analytical Techniques

Samples of the Kolumbo volcanic deposits were acquired with an ROV during 2010 (NA007) and 2011 (NA014) cruises of the Exploration Vessel *Nautilus* (see Figure 1 for sampling locations). Due to the limitations of the ROV robot arm, sampling was restricted to loose clast $<$10 cm in size, but it was possible to obtain samples from the pumice and lava bodies. A total of 15 Kolumbo samples were initially analyzed for major and minor element composition by X-ray fluorescence spectroscopy (XRF) at the University of Rhode Island. Five of these samples and six new samples were subsequently analyzed for trace element and Sr-Nd-Hf-Pb isotope composition at the Vrije Universiteit Amsterdam. For comparison, five samples of the Nea Kameni dacites and Minoan Tuff of Santorini have been included in the sample set (see supporting information for sample details). Pumice and lava samples were cut in smaller pieces with a diamond saw, carefully removing any weathered parts, and subsequently cleaned thoroughly in demineralized water in an ultrasonic bath. After drying, pumice samples were lightly crushed in an agate pestle and mortar after which fragments of mafic enclaves were carefully removed. For one K2 pumice sample, a sufficient amount of enclave fragments (ca. 10 g) was separated to allow geochemical characterization. Lava samples were reduced in size using a hardened-steel jawcrusher. The lightly crushed pumice and lava fragments were reduced to a powder using an agate planetary ball mill.

The major element composition of the new samples was determined by XRF on fused glass beads. Sample powders were ignited at 1000 °C for 2 h to determine loss on ignition before being mixed with $Li_2B_4O_7$/$LiBO_2$ mixture (1:4 dilution), fused to a bead at 1150 °C and measured on a Panalytical AxiosMax XRF instrument at the Vrije Universiteit Amsterdam. All XRF results are reported on a volatile-free basis normalized to 100 wt.% with Fe expressed as total ferrous iron (FeO*). Replicate analyses of samples previously analyzed at the University of Rhode Island indicate that results from the two laboratories are within analytical uncertainty ($<$3% relative standard deviation for major elements). Aliquots of selected samples were subsequently digested in PTFE bombs in a HF/HNO_3 mixture after which trace element concentrations were measured

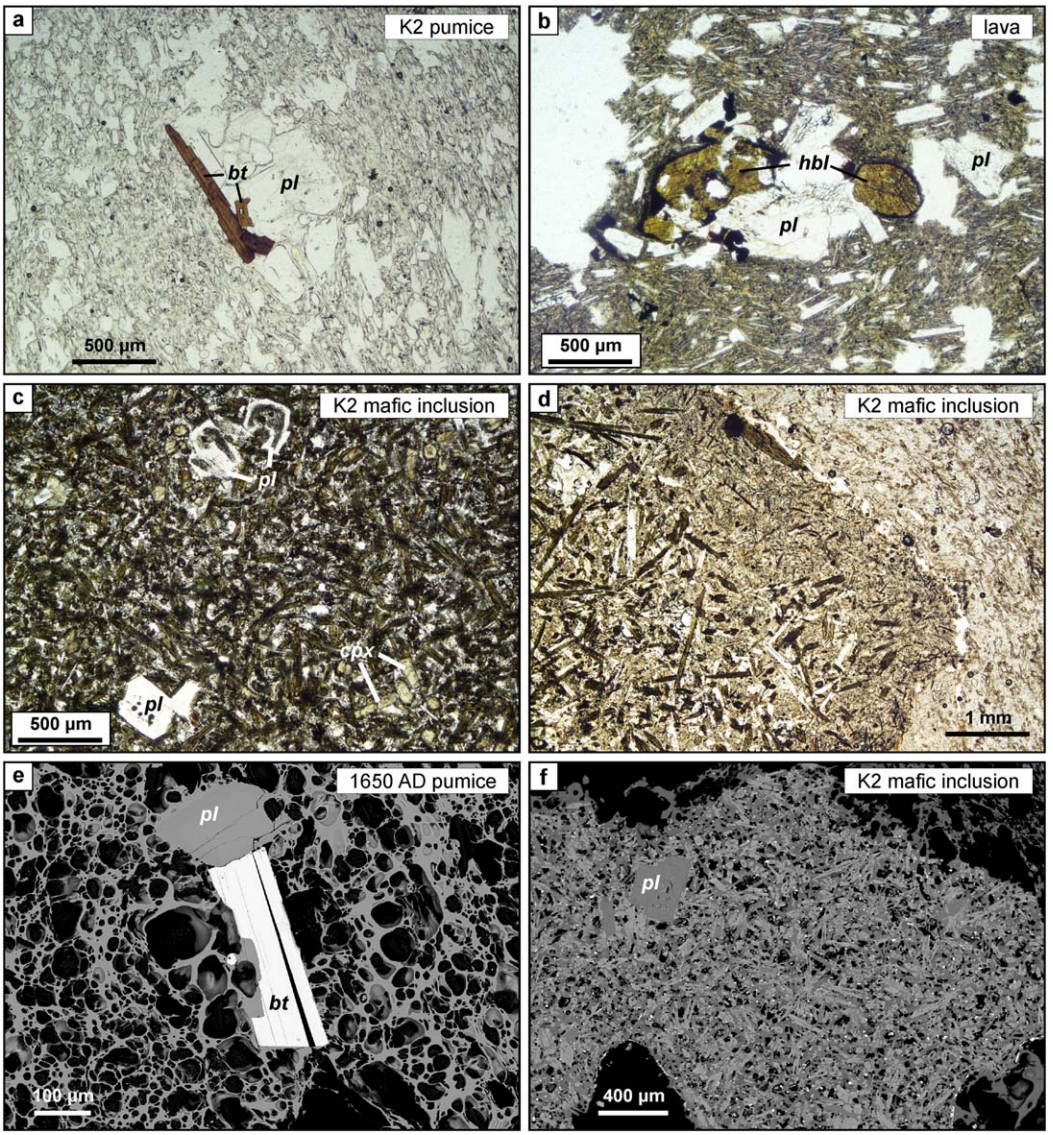

Figure 2. Typical examples of the Kolumbo volcanic rocks: photomicrographs in (a-d) plain polarized light and (c-f) backscattered electron (BSE) images; (a) K2 pumice sample, showing a cluster of euhedral plagioclase and biotite phenocrysts in a glassy, vesicular matrix; (b) Kolumbo lava sample with a microlite groundmass with seriate texture plagioclase and two partly resorbed hornblende phenocrysts with opacite rims; (c) Mafic inclusion in a K2 pumice sample with plagioclase and clinopyroxene in a quench texture groundmass of acicular hornblende and plagioclase. The plagioclase crystal in the top-center has a pronounced sieve textured core; (d) The fine-grained, chilled margin of a mafic enclave in the K2 pumice indicates rapid quenching as a result of its incorporation in a cooler silicic host; (e) 1650 AD pumice sample with a euhedral biotite and plagioclase phenocryst in a glassy, vesicular matrix; (f) The same mafic inclusion as shown in Figure 2c in which acicular hornblende (light grey) and plagioclase (mid grey) display a quenched, spherulitic texture with diktytaxitic voids (black). White specks are Fe-Ti-oxides. Note the absence of a chilled margin in this inclusion, in contrast with the one shown in Figure 2d.

by ICPMS and Sr-Nd and Hf isotopes by TIMS and MC-ICPMS respectively, following the procedures outlined in *Klaver et al*. [2015]. Over the course of this study, standard reference material (SRM) 987 yielded $^{87}Sr/^{86}Sr = 0.710251 \pm 0.000030$ (2 SD, n = 6), in-house Nd reference material CIGO yielded $^{143}Nd/^{144}Nd = 0.511331 \pm 0.000008$ (2 SD, n=6; equivalent to a value of 0.511841 for La Jolla [*Griselin et al*., 2001]) and the JMC-475 Hf standard reagent gave $^{176}Hf/^{177}Hf = 0.282169 \pm 0.000009$ (2 SD, n = 19). Lead isotopes were measured by TIMS using a ^{207}Pb-^{204}Pb double spike to correct for instrumental mass fractionation [*Klaver et al*., 2016b], giving a reproducibility for SRM 981 of $^{206}Pb/^{204}Pb = 16.9412 \pm 0.0004$, $^{207}Pb/^{204}Pb = 15.4987 \pm 0.0003$ and $^{208}Pb/^{204}Pb = 36.7219 \pm 0.0010$ (2 SD, n = 5). Results for external standards AGV-2 and BCR-2 overlap with recommended values and are listed in the online supporting information.

Mineral and glass compositions of a K2 pumice and 1650 AD pumice sample were determined using JEOL JXA-8530F electron probe microanalyzer at the Dutch National Geological Facility, Utrecht University, at an acceleration voltage of 15 kV. For biotite, amphibole and pyroxene analyses, a beam current of 20 nA and focused spot were used. To prevent Na loss, the beam current was lowered to 10 nA and a spot size of 5 μm was employed for glass and plagioclase analyses. Results were normalized using an online φ(rZ) correction. All EMP results are provided in the online supporting information.

4. Results

4.1. Petrography of the Kolumbo Suite

The two pumice deposits exposed in the Kolumbo crater, the K2 and 1650 AD pumices, have similar petrographic features but are readily distinguishable. The 1650 AD products are white pumices with 40–70% round to elongated vesicles (<5 mm) and <5% plagioclase and biotite phenocrysts (Figure 2; see also *Cantner et al.* [2014]), while the K2 pumices are grey and contain considerably fewer and smaller vesicles (<1 mm). Both pumice units have a holohyaline groundmass and plagioclase is the dominant phenocryst phase (1–3 vol.%) along with common euhedral biotite (Figure 2). Fe-Ti-oxides comprise <1 vol.% and orthopyroxene, quartz and amphibole are rare phenocryst phases. Zircon and apatite occur as accessory phases that are hosted predominantly in plagioclase. Both the K2 and 1650 AD pumices contain cm-sized mafic inclusions (generally 0.2–2 cm) with a quench texture of acicular plagioclase and amphibole and larger phenocrysts (up to 500 μm) of plagioclase, clinopyroxene and rare amphibole (Figure 2). Plagioclase phenocrysts in the mafic inclusions display a wide variation in textures and often have sieve textured cores. The contacts between the inclusions and the host pumice are invariably sharp, but the mafic inclusions vary from angular to rounded; chilled margins are generally better developed in the rounded inclusions. The presence of chilled margins and the quenched, sometimes spherulitic, amphibole-plagioclase texture suggest that these inclusions originate as mafic enclaves that rapidly crystallized upon intrusion in the cooler host magma.

Several poorly defined intrusive bodies in the lower parts of the Kolumbo crater probably represent lavas or dykes intruded in the pumice deposits [*Hübscher et al.*, 2015] and are therefore referred to as lava samples. The samples of the lava bodies typically have a porphyritic texture of plagioclase, clinopyroxene, amphibole, Fe-Ti-oxide and rare orthopyroxene phenocrysts set in a fine plagioclase microlite groundmass (Figure 2b). Amphibole in the lavas generally has an opacite reaction rim as a result of decompression and some plagioclase crystals display complex oscillatory zonation patterns that are not commonly seen in the pumices.

4.2. Glass Geochemistry

The major element compositions of the Kolumbo K2 and 1650 AD glasses are shown in two discrimination diagrams in Figure 3. Our results for the 1650 AD pumice agree well with those reported by *Cantner et al.*

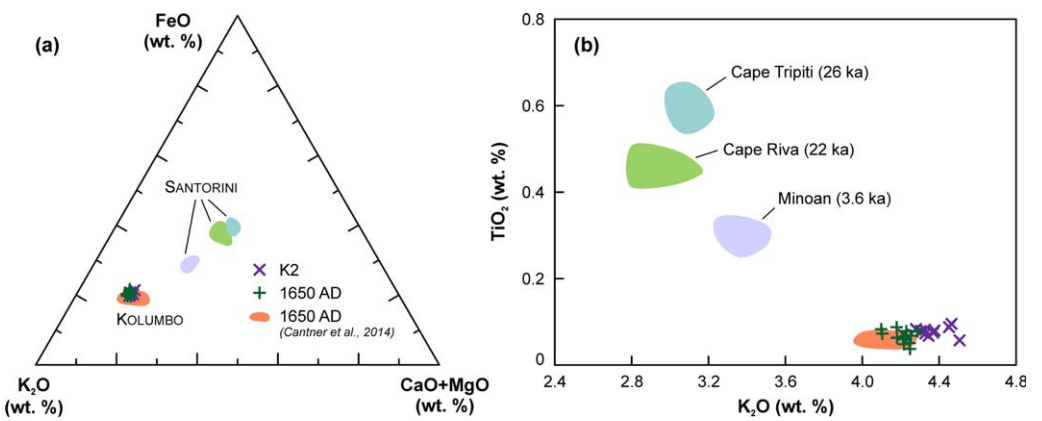

Figure 3. Glass compositions for the K2 and 1650 AD pumice samples: (a) FeO – K_2O – CaO+MgO ternary diagram; (b) TiO_2 versus K_2O diagram. Data for the 1650 AD pumice from *Cantner et al.* [2014] are included (orange field). Glass compositions of eruptive products from the three most recent major Plinian eruptions from Santorini (Cape Tripiti, Cape Riva, Minoan) are shown for reference; data are from *Vinci* [1985], *Wulf et al.* [2002], *Aksu et al.* [2008] and *Fabbro et al.* [2013]. All analyses are recalculated on a volatile-free basis normalized to 100%.

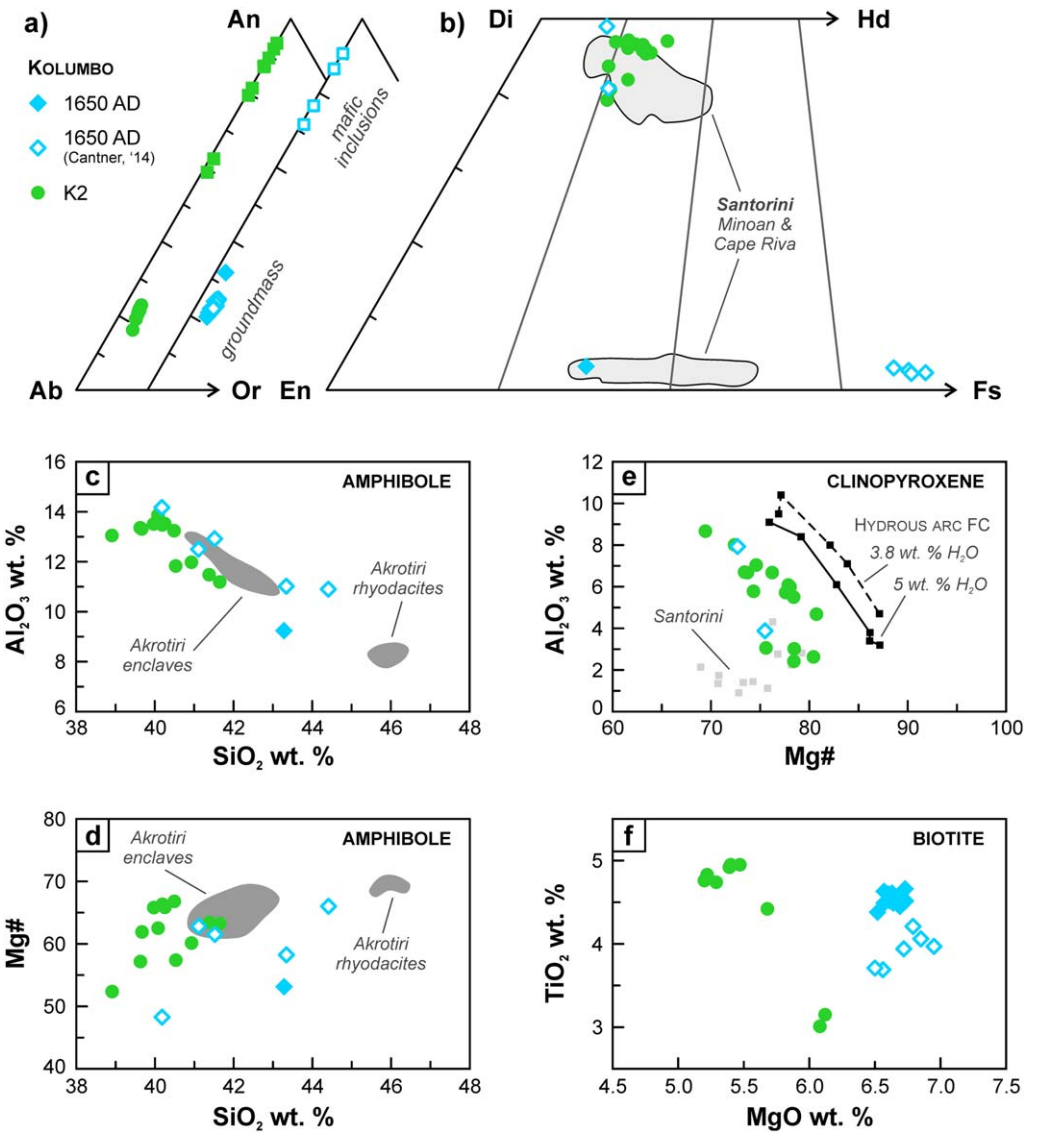

Figure 4. Compositions of (a) plagioclase, (b, e) pyroxene, (c, d) amphibole, and (f) biotite in K2 and 1650 AD pumice samples compared with Santorini Minoan and Cape Riva mineral data (light grey squares and fields [*Huijsmans*, 1985; *Cottrell et al*., 1999; *Druitt et al*., 1999]. Data for the 1650 AD pumices are from *Cantner et al*. [2014] and are shown as open symbols. Also included in Figures 4c and 4d is the range of amphibole compositions in the Akrotiri rhyodacites and enclaves on Santorini [*Mortazavi and Sparks*, 2004]. The composition of clinopyroxene formed during hydrous crystallization experiments of primitive arc magmas is shown for reference in Figure 4e [*Müntener et al*., 2001].

[2014], apart from Na_2O contents that are ~0.4 wt.% lower in our data set. This offset could be the result of Na-loss during our analyses, despite our best efforts to minimize Na-loss by using a larger spot size and lower beam current. As is evident from Figure 3, there is no discernible difference in major elements other than Na_2O between our results and those from *Cantner et al*. [2014].

Both K2 and 1650 AD glasses are rhyolitic in composition with SiO_2 contents of ~75.5 wt.% (on a volatile-free basis). The two deposits cannot be distinguished on the basis of major element composition of the pumice glasses as the average compositions for the two samples are within analytical uncertainty (2 SD), although it could be argued that the K_2O content of the K2 pumice is somewhat higher (Figure 3b). The Kolumbo glasses are clearly different from the glass compositions of products from the last three major Plinian eruptions of Santorini (Figure 3). In the recent volcanological record of Santorini, the 3.6 ka Minoan eruption has the most silicic glass composition: 73.4 ± 0.4 wt.% SiO_2 [*Federman and Carey*, 1980; *Vinci*, 1985]. The 26 ka Cape Tripiti [*Fabbro et al*., 2013] and 22 ka Cape Riva [*Vinci*, 1985; *Wulf et al*., 2002]

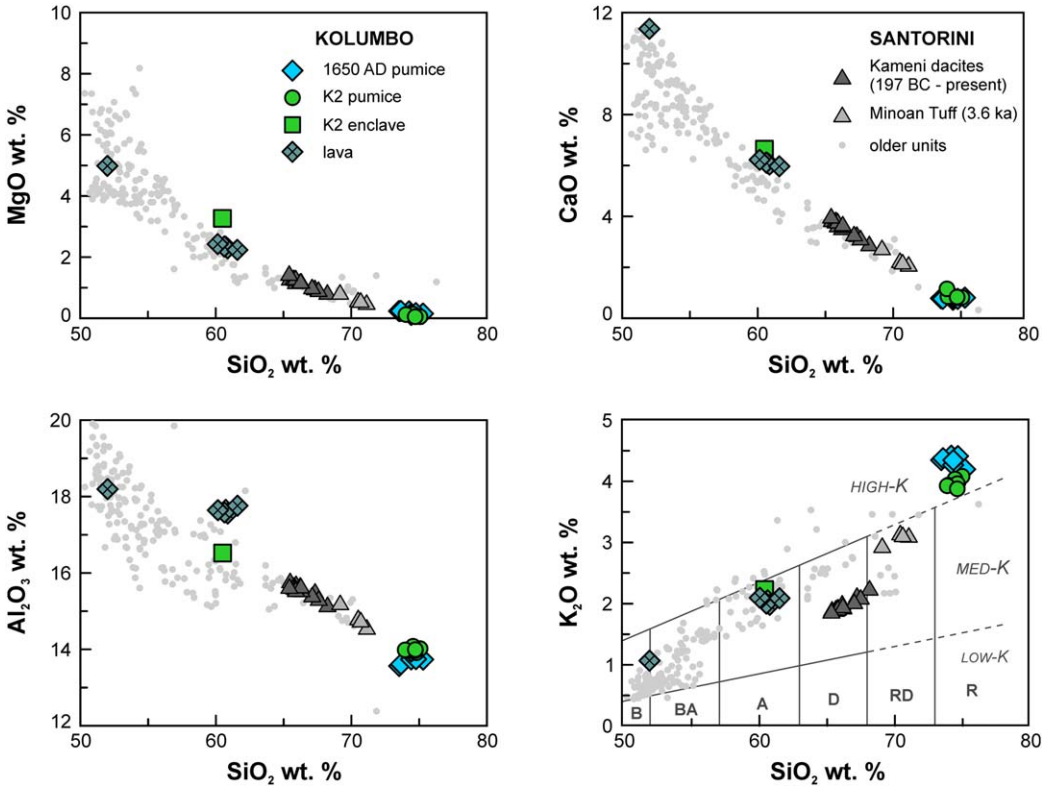

Figure 5. Whole rock major element variation diagrams for Kolumbo compared with Santorini [*this study; Druitt et al.*, 1999; *Zellmer et al.*, 2000; *Mortazavi and Sparks*, 2004; *Bailey et al.*, 2009; *Kirchenbaur et al.*, 2012; *Fabbro et al.*, 2013; *Druitt*, 2014; *Klaver et al.*, 2016a]. For Santorini, the 197 BC to 1950 AD Kameni dacites (dark grey triangles) and 3.6 ka Minoan Tuff (light grey triangles), which are roughly synchronous with the Kolumbo deposits, are highlighted. The K_2O versus SiO_2 diagram is after *Le Maitre et al.* [1989].

eruptions have both deposited pumices with lower glass SiO_2 contents. Hence, the Kolumbo glasses are significantly more evolved than those erupted during the recent explosive events on Santorini.

4.3. Mineral Geochemistry

The major element composition of minerals in the 1650 AD and K2 pumice is shown in Figure 4 and compared with data for Santorini. Plagioclase phenocrysts in the 1650 AD and K2 pumices are similar in composition with An% between 19 and 22. Higher An% plagioclase in these samples is found in the mafic inclusions in which plagioclase cores range up to 93 An%. Acicular amphibole in these mafic inclusions is unusually SiO_2-poor magnesiohastingsite to tschermakitic pargasite with Mg# (assuming total Fe as Fe^{2+}) between 50 and 70 and 11–14 wt.% Al_2O_3. In comparison, the Akrotiri rhyodacites, the only unit on Santorini with a significant proportion of hornblende (see section 5.1.2), show a bimodal distribution of amphibole compositions with more SiO_2-rich and Al_2O_3-poor amphibole residing in the rhyodacitic host and more SiO_2-poor and Al_2O_3-rich amphibole present in the mafic enclaves (Figure 4) [*Mortazavi and Sparks*, 2004]. Kolumbo amphibole roughly overlaps in composition with amphibole in the Akrotiri enclaves. Clinopyroxene in mafic inclusions and mafic crystal clots in the K2 pumice has high Al_2O_3 contents up to 9 wt.% at Mg# between 69 and 81, with generally lower Al_2O_3 contents in crystal rims. Biotite compositions in the K2 and 1650 AD pumice are distinct and can be differentiated on the basis of higher MgO content in 1650 AD biotites (6.5–7.0 wt.% compared to 5.0–6.2 wt.% in the K2 pumice).

4.4. Whole Rock Geochemistry

The whole rock geochemical composition of the Kolumbo suite is shown in Figures 5–8 where the data are compared with a compilation of data for the volcanic products of Santorini, which includes the new data for the Nea Kameni dacites and Minoan Tuff (see Figure 5 for data sources). To facilitate comparison with recent magmatism on Santorini that is coeval with the eruption of the 1650 AD pumices, Nea Kameni dacite

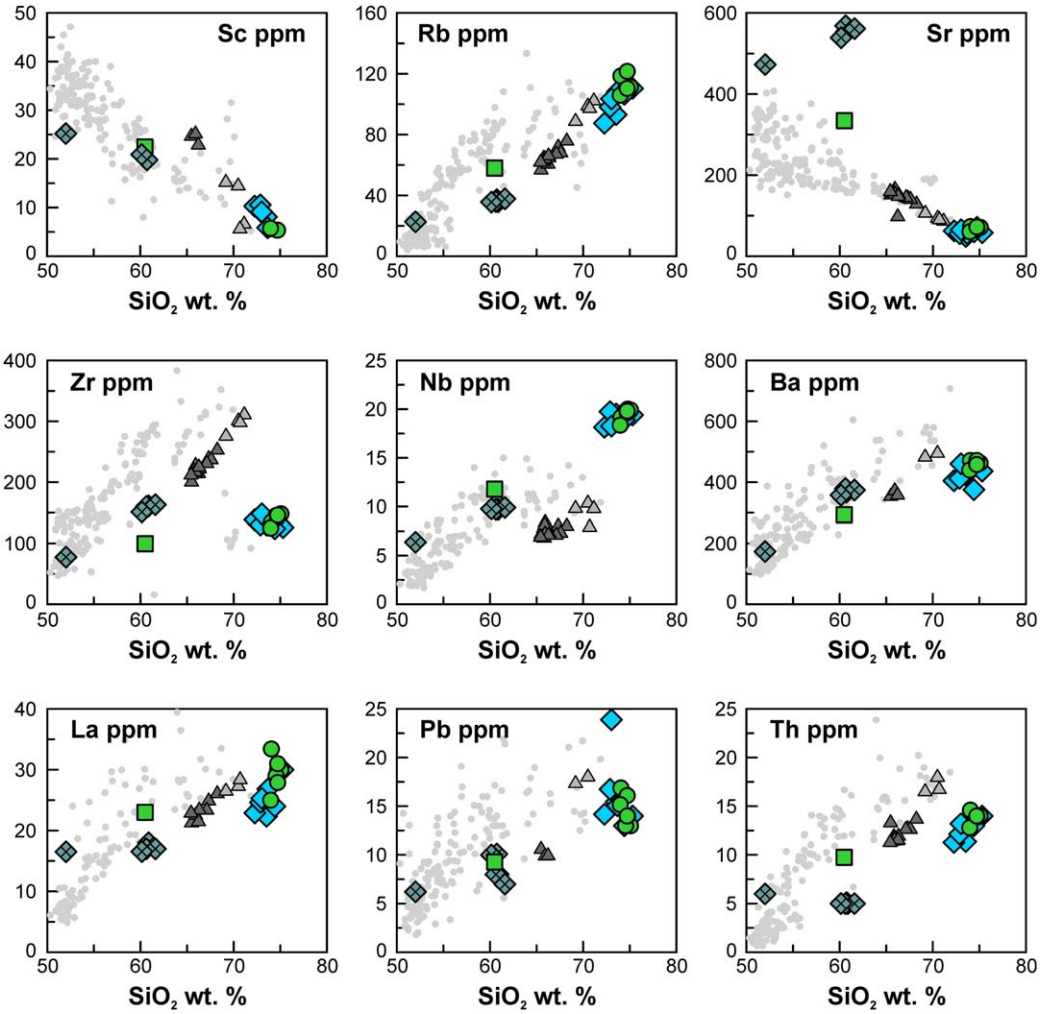

Figure 6. Variation diagrams of selected trace elements versus SiO_2 for the Kolumbo sample suite in comparison with the range of Santorini volcanic products. For Santorini, the recent Kameni dacites (dark grey triangles) and Minoan Tuff (light grey triangles) are highlighted. Symbols and data sources as in Figure 5.

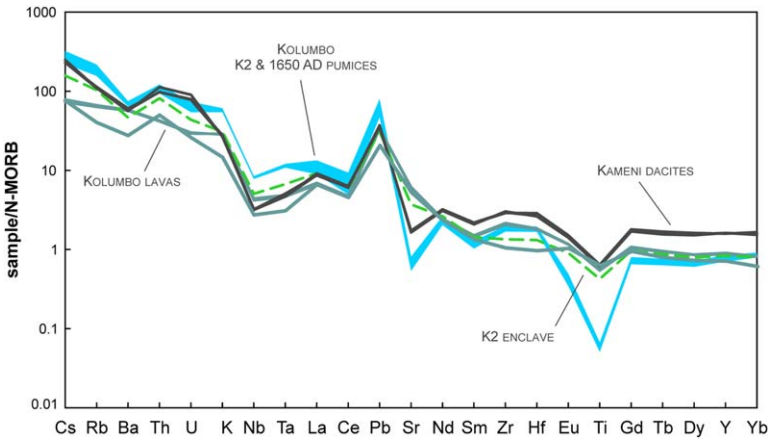

Figure 7. N-MORB normalized multielement abundance diagram of the Kolumbo samples in comparison with the recent Santorini Kameni dacites; N-MORB values from *Sun and McDonough* [1989]. The light blue field represents the total variation of the K2 and 1650 AD pumices combined; these two pumice suites are indistinguishable in this diagram.

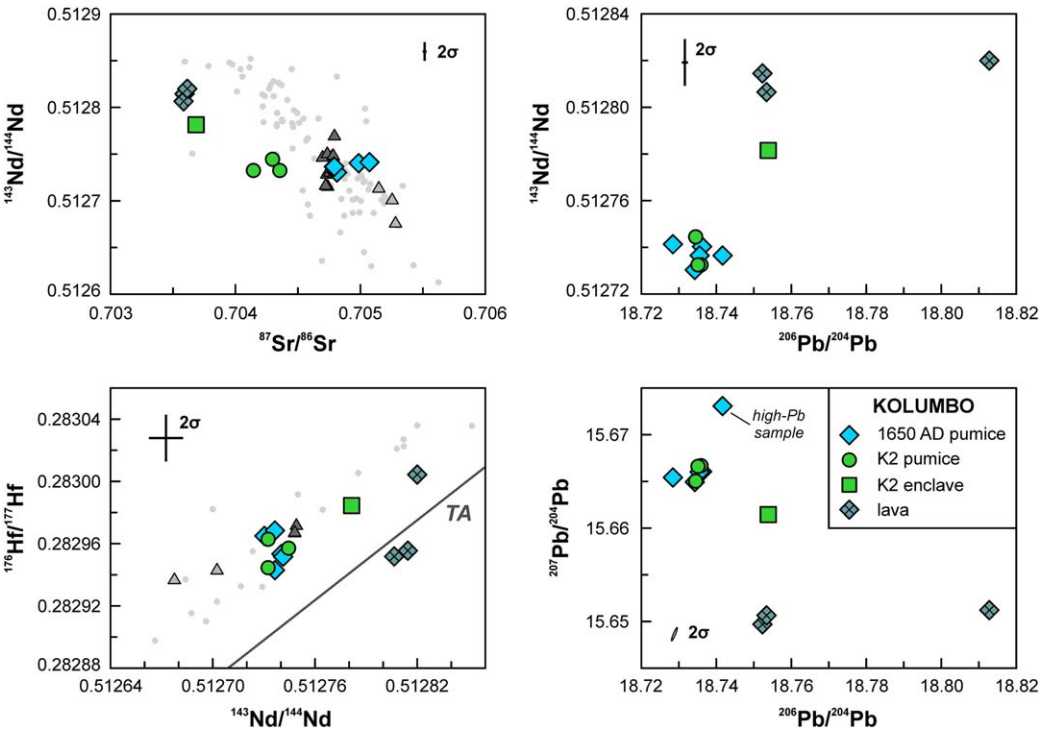

Figure 8. Sr-Nd-Hf-Pb isotope diagrams for Kolumbo compared to data for Santorini (grey circles) with the recent Kameni dacites (dark grey triangles) and Minoan Tuff (light grey triangles) highlighted. Data sources as in Figure 5). For scaling purposes, the Santorini data ($^{206}Pb/^{204}Pb > 18.8$) are omitted from the Pb diagrams, but are shown in Figures 10 and 12. The terrestrial array (TA) in the $^{176}Hf/^{177}Hf$ versus $^{143}Nd/^{144}Nd$ diagram is from *Vervoort et al*. [2011].

and Minoan Tuff samples are highlighted in all figures. The full geochemical data for the Kolumbo samples, as well as the new Santorini data, are provided in the online supporting information.

4.4.1. Major and Trace Elements

Figures 5 and 6 show the variation of a selection of major and trace elements in the Kolumbo suite. The 1650 AD and K2 pumices are rhyolites with 72 to 74 wt.% SiO_2. Compared to the Minoan Tuff, which is the most evolved unit on Santorini with 69–71.5 wt.% SiO_2 [e.g., *Druitt et al*., 1999; *Druitt*, 2014], the Kolumbo pumices have higher SiO_2, Na_2O and K_2O, and lower MgO, FeO*, TiO_2, Al_2O_3 and CaO contents (Figure 5). Kolumbo lavas are basaltic to andesitic in composition and overlap with Santorini for MgO and K_2O contents, but the andesitic lavas are characterized by a higher Al_2O_3 concentration (17.7 wt.%). The silica content of the mafic enclave in a K2 pumice sample is similar to the Kolumbo lavas, but is distinct in MgO, Al_2O_3 and trace element concentrations. In terms of major element composition, the K2 and 1650 AD pumices are similar but not identical. The 1650 AD pumices are marginally lower in SiO_2 and Al_2O_3, but Na_2O and K_2O contents are the main difference: K2 pumices have lower alkali concentrations, even though the K2 glasses are characterized by higher K_2O contents (Figure 3).

Trace element concentrations are mostly uniform for the two pumice groups except for a more pronounced difference in Sc and Rb contents (Figure 6). A single 1650 AD pumice sample retrieved from the hydrothermal field on the crater floor (Figure 1c) has an anomalously high Pb content (23 ppm, ~8 ppm higher than the other samples) that is likely related to hydrothermal alteration. The trace element characteristics of the Kolumbo suite are distinct from the large variation shown by the Santorini volcanic rocks. The most notable differences are lower Zr, La and Th contents in the Kolumbo lavas and pumices compared to Santorini. In contrast, Sr contents are much higher in the Kolumbo andesitic lavas compared to Santorini andesites (ca. 550 ppm versus 200–300 ppm respectively). Niobium contents of the Kolumbo pumices (18–20 ppm) are elevated compared to both the Santorini rhyolites and Kameni dacites (<13 ppm), although the pumices fall on an extrapolated trend defined by the less evolved Santorini samples. Whereas the Zr content of the Kolumbo pumices is lower than in the Minoan pumice (ca. 130 versus 300 ppm respectively), it is similar to Santorini's hornblende-bearing Akrotiri rhyodacites with ca. 100 ppm Zr at 69–71 wt.% SiO_2 [*Mortazavi and*

Sparks, 2004]. The trace element data furthermore show that the Kameni dacites are also distinct from the main Santorini trend and generally have lower trace element abundances than the older volcanic units of Santorini at similar SiO_2 content [e.g., *Huijsmans et al*., 1988; *Zellmer et al*., 2000].

The difference between the Kolumbo pumices and Kameni dacites is highlighted in an N-MORB normalized multi-element abundance diagram (Figure 7). Both sample suites have a trace element pattern typical of subduction zone magmas with negative Nb-Ta and Ti anomalies, pronounced LILE over HFSE enrichment and a large, positive Pb anomaly compared to N-MORB. The Kameni dacites have higher concentrations of less incompatible elements, such as middle to heavy rare earth elements (MREE and HREE), Zr and Y, while LILE concentrations are roughly similar. In addition, both the Kolumbo and the Kameni samples have a negative Ba anomaly and a small but distinct positive Zr-Hf anomaly relative to Sm.

4.4.2. Sr-Nd-Hf-Pb Isotopes

The Kolumbo pumices display a limited range in Pb isotope compositions ($^{206}Pb/^{204}Pb = 18.725–18.745$) that is lower compared to Santorini ($^{206}Pb/^{204}Pb = \sim18.8–19.0$; Figures 8, 10 and 12). In terms of $^{87}Sr/^{86}Sr$, $^{143}Nd/^{144}Nd$ and $^{176}Hf/^{177}Hf$, there is more overlap between Kolumbo and the range displayed by the Santorini volcanic rocks. Within the Kolumbo suite, the lavas and K2 enclave have lower $^{87}Sr/^{86}Sr$, $^{207}Pb/^{204}Pb$ and $^{208}Pb/^{204}Pb$ and higher $^{143}Nd/^{144}Nd$ and $^{176}Hf/^{177}Hf$, and are thus closer to depleted mantle compared to the pumices, but $^{206}Pb/^{204}Pb$ is higher in these samples and the basaltic lava $^{206}Pb/^{204}Pb = 18.815$ overlaps with the least radiogenic Santorini values (Figures 10 and 12). The andesitic lava samples fall on the terrestrial Nd-Hf isotope array of *Vervoort et al*. [2011], whereas the Kolumbo basaltic lava, pumices and Santorini samples have lower $^{143}Nd/^{144}Nd$ for a given $^{176}Hf/^{177}Hf$. The K2 and 1650 AD pumices have identical Nd, Hf and Pb isotope compositions with the exception of two 1650 AD pumices; one of which has a higher Pb content (Figure 6) and more radiogenic Pb isotope composition whilst the other has lower $^{206}Pb/^{204}Pb$ and $^{208}Pb/^{204}Pb$ but overlapping $^{207}Pb/^{204}Pb$. In terms of $^{87}Sr/^{86}Sr$, however, the two Kolumbo pumice suites show considerable variation and the 1650 AD pumices have a more radiogenic composition (0.7048–0.7051) than the K2 pumices (0.7042–0.7044). As $^{87}Sr/^{86}Sr$ shows a well-defined positive correlation with Na_2O content for the rhyolitic pumices (not shown), the higher $^{87}Sr/^{86}Sr$ in the 1650 AD pumices likely reflects seawater addition to the more vesicular 1650 AD pumices.

5. Discussion

5.1. Comparison Between Kolumbo and Recent Santorini

The occurrence within the same extension-related basement fault zone along the CSK tectonic line and short distance between the two volcanic centers (15 km from the center of Santorini caldera to the center of the Kolumbo crater; Figure 1) suggest that Kolumbo and Santorini could be different surface expressions of the same volcanic system. This is supported by the proposed lateral extension of a shallow (5–7 km) crustal hot zone underneath Kolumbo toward the magmatic system of Santorini [*Dimitriadis et al*., 2010]. To investigate a possible relationship between the crustal plumbing system of Santorini and Kolumbo, we will address some first-order observations that arise from a comparison of the petrographic and geochemical characteristics of the Kolumbo suite and recent Santorini products.

5.1.1. A Present-Day, Shallow Connection?

The 1650 AD eruption of Kolumbo occurred contemporaneously with the intermittent volcanic activity in the center of the Santorini caldera over the last ~2 kyr. Dacitic lava flows erupted from the Nea Kameni vent in the Santorini caldera in 1570–1573 AD and 1707–1711 AD [*Druitt et al*., 1999], hence enveloping the 1650 AD eruption of Kolumbo. The rhyolitic 1650 AD pumices are different in terms of petrography and geochemistry from the Kameni dacites, which are very homogeneous and do not display significant temporal variation over the last ~2 kyr [*Barton and Huijsmans*, 1986; *Zellmer et al*., 2000]. In contrast with the abundance of biotite and amphibole in the Kolumbo pumices and enclaves, the Kameni dacites are characterized by an anhydrous mineral assemblage dominated by plagioclase, clinopyroxene and orthopyroxene, and a complete absence of amphibole in quenched mafic enclaves hosted in the dacites [*Martin et al*., 2006]. The geochemical differences are even more pronounced; the Kolumbo pumices are significantly more evolved at 72–74 wt.% SiO_2 and have higher alkali element abundances (Figure 5), which is emphasized by distinct trace element patterns (Figures 6 and 7) and isotope compositions (Figure 8). Hence, it is highly unlikely that the 1650 AD pumice are derived from the same shallow magmatic system from which the Kameni dacites are tapped. This is supported by the distinct He isotope composition of gasses emitted

from vents in the Kameni islands and the Kolumbo hydrothermal system (3–4 Ra and 7.0–7.1 Ra, respectively) [*Rizzo et al*., 2016]. A scenario in which the 1650 AD pumices represent evolved residual magma of the 3.6 ka rhyodacitic Minoan eruption can also be precluded on the basis of large trace element and isotope differences (Figures 6 and 8). Although $^{87}Sr/^{86}Sr$, $^{143}Nd/^{144}Nd$ and $^{176}Hf/^{177}Hf$ values overlap, in particular lower $^{206}Pb/^{204}Pb$ in the Kolumbo pumices compared to the recent Santorini products (Figure 10) strongly argues against a direct genetic relationship between the Minoan Tuff or Kameni dacites and the 1650 AD pumice. On the basis of these observations, it can be concluded that the Kolumbo 1650 AD pumice is not related to the recent Santorini volcanic products and is derived from a reservoir with geochemically distinct magma. Given the strong similarity in petrography and geochemistry of the K2 and 1650 AD pumices, it is likely that the K2 pumices are derived from the same distinct magmatic system as the 1650 AD deposits and are also unrelated to Santorini. Hence, the new geochemical data do not support the proposed connection between the magmatic systems of Kolumbo and Santorini [*Dimitriadis et al*., 2010]. Whether the Kolumbo and Santorini magmas are derived from the same mantle source but have obtained their geochemical differences through distinct crustal differentiation processes, is discussed in sections 5.2 and 5.3.

5.1.2. Amphibole and Biotite in the Kolumbo Suite

The main petrographic feature of the Kolumbo suite is the ubiquitous presence of biotite in the K2 and 1650 AD pumices. Amphibole is a common phase in the lavas and enclaves, and occurs sporadically in the pumices. Both these phases are rare in Santorini; biotite is absent altogether and amphibole occurs only as a significant phenocryst phase in the >550 ka Akrotiri rhyodacites, the oldest volcanic unit on Santorini that is distinct from all younger Santorini volcanic deposits in terms of petrography and geochemistry [*Mortazavi and Sparks*, 2004]. In the younger Santorini deposits, trace amounts of amphibole occur in Lower Pumice 2 [*Gertisser et al*., 2009], amphibole occurs as rare inclusions in orthopyroxene in the Minoan pumice [*Cottrell et al*., 1999] and hornblende-bearing microphenocryst-rich pumices and hornblende-diorites were coerupted with the Minoan Tuff [*Druitt*, 2014].

Despite the common absence of amphibole phenocrysts in arc lavas worldwide, the vast majority of arc volcanic suites display geochemical evidence for cryptic amphibole fractionation [*Davidson et al*., 2007, 2013; *Smith*, 2014] and the role of amphibole as a major phase in controlling the differentiation of hydrous arc magmas is suggested by a number of experimental studies [e.g., *Sisson and Grove*, 1993; *Alonso-Perez et al*., 2009]. Figure 9 displays the variation of Y and Dy/Yb with SiO_2 content. As Y and Dy are compatible in amphibole but largely incompatible in a typical anhydrous assemblage (Pl+Cpx±Ol±Opx), these parameters are indicative of the presence of amphibole as a fractionating phase [e.g., *Davidson et al*., 2007]. The less evolved Santorini volcanic rocks (<65 wt.% SiO_2) are characterized by a general increase in Y content and subhorizontal Dy/Yb that is consistent with largely amphibole-free differentiation, as also concluded by *Mortazavi and Sparks* [2004] and *Elburg et al*. [2014]. Only the Santorini (rhyo)dacites (>65 wt.% SiO_2) are characterized by decreasing Y contents and Dy/Yb with SiO_2, suggesting a modest amphibole control in the most evolved rocks [*Elburg et al*., 2014]. The Kolumbo pumices have subchondritic Dy/Yb and low Y

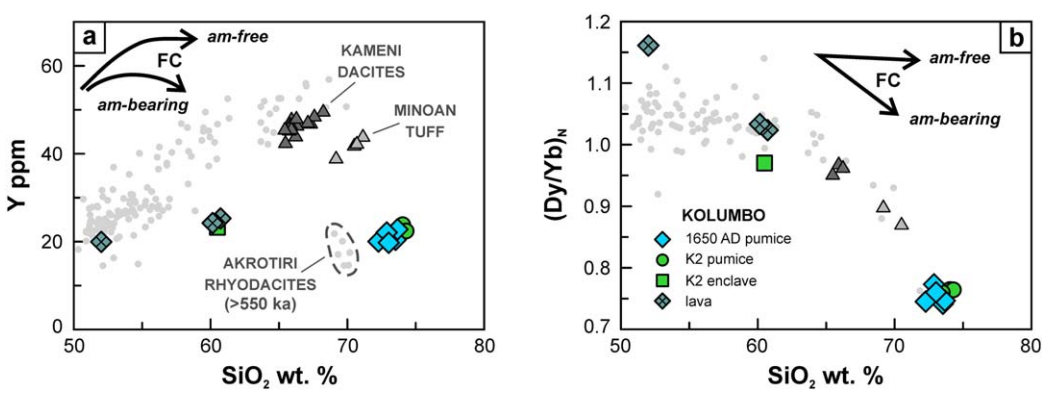

Figure 9. (a) Yttrium and (b) chondrite-normalized Dy/Yb versus SiO_2 for the Kolumbo suite in comparison with Santorini (small grey circles) indicating the control of amphibole on the differentiation trends of Kolumbo. Schematic fractional crystallization (FC) trends with and without amphibole are shown for reference (based on e.g., *Mortazavi and Sparks* [2004], *Davidson et al*. [2007] and *Elburg et al*. [2014]). Note the anomalously low Y content in the >550 ka Akrotiri rhyodacites compared to the main Santorini trend; too few Dy/Yb data are available for the Akrotiri rhyodacites to be shown separately. Data sources as in Figure 5.

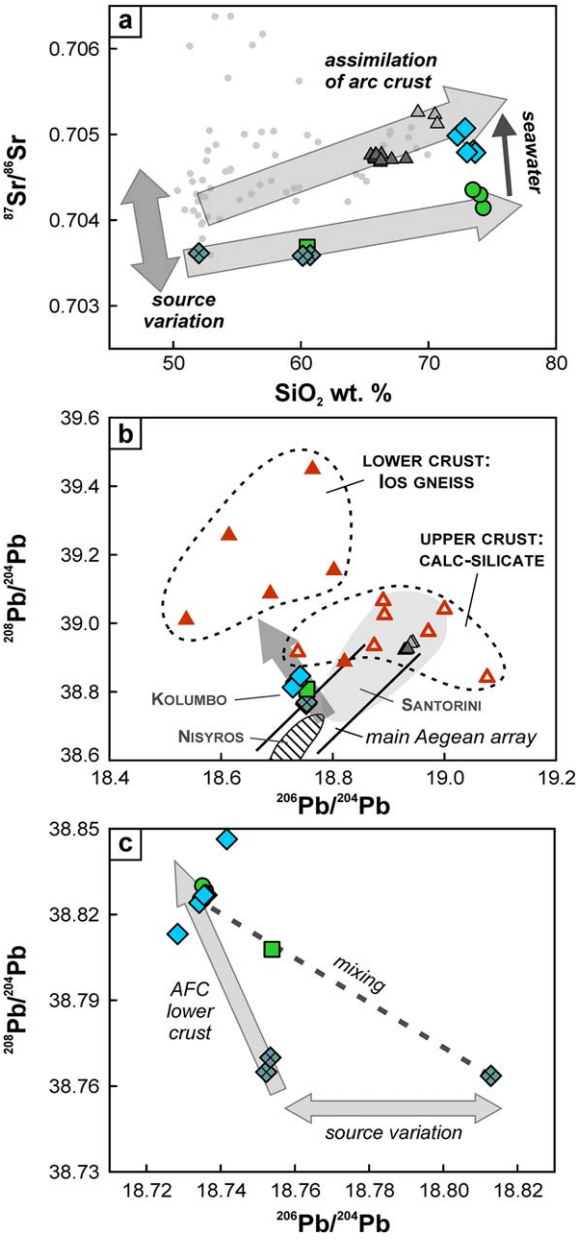

Figure 10. Assimilation of arc crust influences the variation in isotopes in the Kolumbo suite; symbols as in Figure 5; (a) $^{87}Sr/^{86}Sr$ versus SiO_2 diagram shows a moderate increase of $^{87}Sr/^{86}Sr$ with SiO_2 content, which is indicative of open system differentiation and assimilation of basement lithologies. The large variation in $^{87}Sr/^{86}Sr$ of the least evolved samples for Santorini and Kolumbo suggests source heterogeneity, whereas the elevated $^{87}Sr/^{86}Sr$ of the 1650 AD pumices can be explained by seawater addition; (b) $^{208}Pb/^{204}Pb$ versus $^{206}Pb/^{204}Pb$ diagram shows that elevated $^{208}Pb/^{204}Pb$ in the Kolumbo suite can be accounted for by assimilation of or mixing with melts derived from the lower crustal basement as represented by Ios orthogneisses. The main Aegean array is defined by Santorini and Nisyros. Data for Nisyros are from *Buettner et al.* [2005] and *Klaver et al.* [2016a]; (c) close-up of Figure 10b showing the variation of the Kolumbo samples. The K2 enclave falls on a mixing line with the basaltic lava, but the andesitic lavas appear to be more plausible parents to the pumices. See text for further discussion.

contents. Moreover, the large difference in Dy/Yb between the lavas and pumices, high Dy/Yb of the basaltic lava and uniformly low Y contents suggest amphibole control over the entire range in SiO_2 contents rather than derivation from a low-Dy/Yb, low-Y source for the Kolumbo suite. The Kolumbo K2 and 1650 AD pumices overlap in Y content with the >550 ka amphibole-bearing Akrotiri rhyodacites. Due to the lack of high-quality Dy and Yb data, however, it is not possible to unequivocally distinguish between amphibole fractionation and other processes leading to low Y contents in the Akrotiri rhyodacites. Hence, Kolumbo and Santorini are characterized by two contrasting differentiation trends, with Kolumbo showing clear geochemical evidence for a key role of amphibole in its petrogenesis, while Santorini appears to have evolved largely through fractional crystallization of an anhydrous mineral assemblage [e.g., *Huijsmans et al.*, 1988; *Druitt et al.*, 1999] with no evidence for amphibole fractionation at <65 wt.% SiO_2. The point that should be stressed is that the amphibole-present differentiation trend shown by Kolumbo is typical of most arc volcanoes worldwide and that Santorini is the exception [*Elburg et al.*, 2014]. The general absence of amphibole in the Santorini suite is likely the result of crystallization under hotter conditions compared to the Akrotiri rhyodacites and, by inference, Kolumbo [*Druitt et al.*, 1999; *Cadoux et al.*, 2014; *Andújar et al.*, 2015].

5.2. Role of Crustal Contamination in the Evolution of Kolumbo

Contamination of arc magmas through assimilation of wall rock lithologies or mixing with crustal melts is a common process and can have a profound influence on the trace element and isotope composition of these magmas [e.g., *Hildreth and Moorbath*, 1988; *Annen et al.*, 2006; *Bezard et al.*, 2014]. Hence, before discussing potential variation in the Kolumbo and Santorini mantle sources, it is essential to assess the influence of assimilation of arc crust in the Kolumbo suite. Correlation between radiogenic isotopes and indices of magma differentiation such as SiO_2 and MgO are taken as strong evidence for assimilation of arc crust, mainly because variations in recycled crustal components derived from the subducting slab do not readily exert a strong control on the major element geochemistry of arc lavas [*Davidson*, 1987; *Thirlwall et al.*, 1996; *Bezard et al.*, 2014]. Figure 10a displays the variation in $^{87}Sr/^{86}Sr$ with SiO_2 content for the Kolumbo samples in comparison with the range

displayed by Santorini. In the Kolumbo suite, higher $^{87}Sr/^{86}Sr$ in the 1650 AD pumices relative to the K2 samples likely reflects seawater addition. Apart from this secondary effect, the Kolumbo suite shows a general increase of $^{87}Sr/^{86}Sr$ with SiO_2 from the lavas to the K2 pumices. Santorini is also characterized by an increase in $^{87}Sr/^{86}Sr$ with magmatic differentiation, indicative of open-system differentiation and contamination of the magmas by arc crust. This is corroborated by decreasing $^{143}Nd/^{144}Nd$ and $^{176}Hf/^{177}Hf$, and increasing $^{207}Pb/^{204}Pb$ with SiO_2 content for Kolumbo (not shown) and Santorini [e.g., *Druitt et al*., 1999; *Zellmer et al*., 2000].

Given the limited systematic variability in their Sr, Nd or Hf isotope composition, it is not possible to distinguish between different potential assimilants on the basis of these isotope systems. Pb isotopes, on the other hand, have the potential to make a general distinction between assimilation of upper- and lower crust in the Santorini volcanic field. Pre-Alpine orthogneisses that are exposed in a core complex on the island of Ios [e.g., *Thomson et al*., 2009], ca. 20 km N of Santorini and Kolumbo (Figure 1) are characterized by high time-integrated Th/U and have therefore evolved to high $^{208}Pb/^{204}Pb$ and moderate $^{207}Pb/^{204}Pb$ at relatively low $^{206}Pb/^{204}Pb$. These Ios gneisses are generally interpreted to constitute the lower crust of the Santorini volcanic field [e.g., *Bonneau*, 1984; *Druitt et al*., 1999; *Kilias et al*., 2013]. In contrast, the shallow calc-silicate basement that is exposed, for instance, on Mt. Profitis Ilias on Santorini is characterized by higher $^{206}Pb/^{204}Pb$ and lower $^{207}Pb/^{204}Pb$ and $^{208}Pb/^{204}Pb$ (Figure 10b). In a $^{208}Pb/^{204}Pb$ versus $^{206}Pb/^{204}Pb$ diagram, Santorini is situated at the radiogenic end of an array defined by the Aegean arc volcanic rocks [*Elburg et al*., 2014]: the "main Aegean array" in Figure 10b. Upper crustal calc-silicate basement samples overlap in Pb isotope composition with the most radiogenic Santorini samples, suggesting that assimilation of upper crustal material is predominant in Santorini [e.g., *Druitt et al*., 1999; *Elburg et al*., 2014]. The Kolumbo samples, however, project away from the main Aegean array toward higher $^{208}Pb/^{204}Pb$ and the field defined by the lower crustal basement. On this basis, we relate the higher $^{208}Pb/^{204}Pb$, $^{207}Pb/^{204}Pb$ and $^{87}Sr/^{86}Sr$ at lower $^{143}Nd/^{144}Nd$ and $^{206}Pb/^{204}Pb$ of the K2 and 1650 AD pumices, compared to the Kolumbo lavas, to the preferential assimilation of pre-Alpine, lower crustal basement. The involvement of lower crustal basement is uncommon in the Aegean arc and such a signature is absent on Santorini and the eastern volcanic center Nisyros; in the west, the Saronic Gulf volcanic centers also display higher $^{208}Pb/^{204}Pb$ at given $^{206}Pb/^{204}Pb$, but this is coupled to more crustal $^{87}Sr/^{86}Sr$ and $^{143}Nd/^{144}Nd$ [*Elburg et al*., 2014].

Despite that $^{207}Pb/^{204}Pb$ and $^{208}Pb/^{204}Pb$ in the Kolumbo suite are elevated compared to the main Aegean array due to crustal assimilation (Figure 10), these values are lower than the majority of the Santorini samples. Relating the lower $^{206}Pb/^{204}Pb$ of Kolumbo to contamination of primitive Santorini magmas ($^{206}Pb/^{204}Pb > 18.88$) with lower crustal basement is thus inconsistent with $^{207}Pb/^{204}Pb$ and $^{208}Pb/^{204}Pb$ of Kolumbo (Figure 10b). This is supported by the high $^{143}Nd/^{144}Nd$ (0.51282) and low $^{87}Sr/^{86}Sr$ (0.7036) of the Kolumbo lavas that rule out a large degree of contamination. Hence, Pb isotopes indicate that the distinct crustal differentiation trends of Kolumbo and Santorini are the result of the preferential assimilation of lower- and upper crust, respectively, but that this difference in assimilants fails to account for the full Pb isotope variability in primitive Kolumbo and Santorini samples. Substantial variation in $^{206}Pb/^{204}Pb$ (18.750–18.815) and $^{176}Hf/^{177}Hf$ (0.28296–0.28300) at constant $^{207}Pb/^{204}Pb$, $^{208}Pb/^{204}Pb$, $^{87}Sr/^{86}Sr$ and $^{143}Nd/^{144}Nd$ in the Kolumbo lavas is also inconsistent with any plausible assimilant and hence we ascribe this to variation in primary magmas delivered to the magmatic systems of Kolumbo and Santorini, which we will investigate in more detail in the next section.

5.3. A Distinct Source for Kolumbo

5.3.1. HFSE Systematics

The trace element diagrams in Figure 6 highlight that the most pronounced differences between Kolumbo and Santorini are found in the high-field strength elements (HFSE). These variations partly result from contrasting crustal differentiation processes as illustrated by the Zr versus SiO_2 trend in Figure 6. The Kolumbo suite displays a minor decrease in Zr concentrations from the lavas to the pumices that is similar to Santorini's Akrotiri rhyodacites, whereas the other Santorini deposits shows a steady increase in Zr with SiO_2. Niobium systematics display the most striking difference between the evolution trends of Kolumbo and Santorini. Figure 11a illustrates that the Kolumbo suite shows a stronger increase in Nb/Yb with SiO_2 compared to Santorini, consistent with the on average higher Nb contents in the Kolumbo pumices. This diagram again provides strong evidence against a direct relationship between the Kolumbo pumices and the recent Kameni dacites and Minoan Tuff as we envisage that there is no plausible fractional crystallization

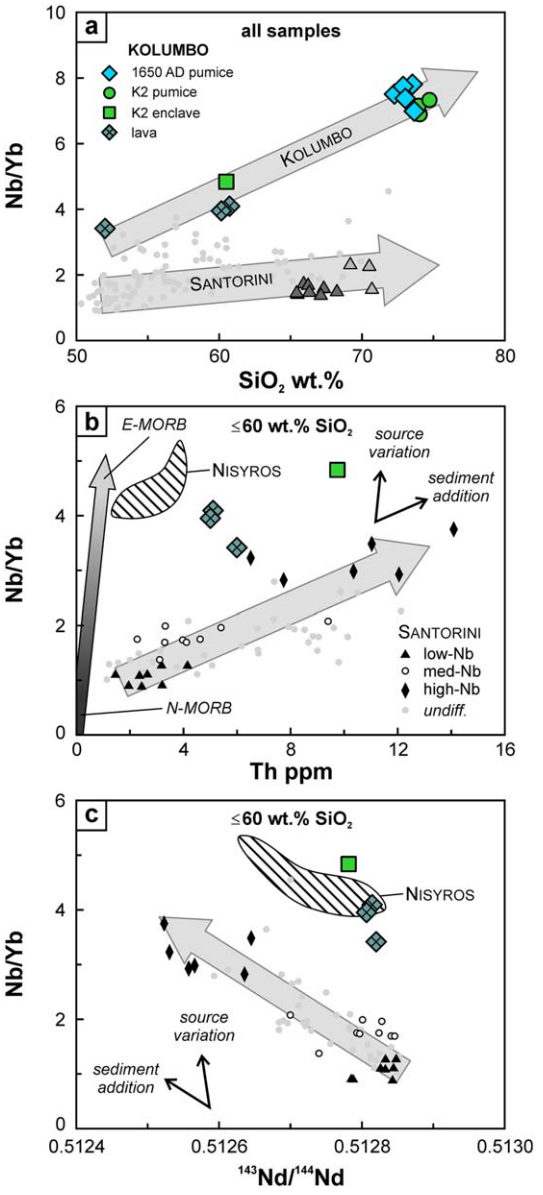

Figure 11. High field strength element variation of Kolumbo and Santorini; (a) Nb/Yb versus SiO_2 diagram showing the stronger increase in Nb/Yb with SiO_2 for Kolumbo compared to Santorini and the difference between the Kolumbo pumices and recent Santorini deposits (symbols as in previous figures). The light grey arrows depict schematic crustal magma differentiation trends; (b) Nb/Yb versus Th diagram for the least evolved (≤60 wt.% SiO_2) Kolumbo lavas, Santorini samples (divided in low-Nb, medium-Nb and high-Nb groups after *Bailey et al.* [2009] and undifferentiated samples), and Nisyros samples [*Klaver et al.*, 2016a]. The shaded grey arrow shows the variation in Atlantic MORB (compilation of *Arevalo and McDonough* [2010]). Nb/Yb increases from N-MORB to E-MORB while Th content only shows a small increase. Source variation and subducted sediment addition trends are based on the MORB array and variations in primitive Santorini basalts. Relatively low Th contents suggest that the Kolumbo lavas have not acquired high Nb/Yb through sediment addition as in the Santorini high-Nb group, but through derivation from a distinct source with HFSE systematics similar to Nisyros; (c) Nb/Yb versus $^{143}Nd/^{144}Nd$ diagram for the least evolved samples supports derivation of the Kolumbo suite from a source distinct from Santorini. Kolumbo $^{143}Nd/^{144}Nd$ is similar to Nisyros but different from the Santorini high-Nb group. See text for further discussion.

process that can produce such a marked increase in Nb/Yb at similar SiO_2 content. Differences in fractionating mineral assemblages are the likely explanation for the sharp increase in Nb/Yb with SiO_2 as well as with Th (Figure 11b) in the Kolumbo suite compared to Santorini. Although the presence of amphibole has imparted a distinct geochemical fingerprint on the Kolumbo suite (see section 5.1.2), the partition coefficient for Nb in amphibole is an order of magnitude higher than for Th [e.g., *Brenan et al.*, 1995] and thus amphibole fractionation should result in a smaller increase in Nb/Yb with Th content. A more plausible explanation is that the Nb content is buffered by abundant Fe-Ti-oxide fractionation in the Santorini suite [e.g., *Huijsmans et al.*, 1988; *Andújar et al.*, 2015]. Alternatively, removal of zircon could present a sink for Th in the Kolumbo suite resulting in the decoupling of Nb/Th, but this fails to explain the high absolute Nb concentrations in the Kolumbo samples.

In addition to the stronger increase in Nb/Yb with SiO_2 for the Kolumbo suite, the Kolumbo lavas appear to have higher Nb/Yb than Santorini samples at any given SiO_2 content. To investigate whether the higher Nb/Yb reflects a source feature or can be explained by the addition of a larger amount of subducted sediments, Nb/Yb is shown against Th content and $^{143}Nd/^{144}Nd$ in Figures 11b and 11c where only the most primitive (≤60 wt.% SiO_2) samples are included. *Bailey et al.* [2009] identified three separate magmatic series on Santorini based on the Nb content of the most primitive samples within each suite. On the basis of correlations between Nb content and Sr-Nd-Pb isotopes, with the high-Nb series corresponding to more enriched isotope compositions, the three magmatic series are interpreted as the result of an increasing contribution of recycled sediments from the low-Nb to the high-Nb series [*Bailey et al.*, 2009]. This interpretation is in good agreement with the suggestion of *Kirchenbaur and Münker* [2015] that the HFSE budget in primitive Santorini samples is dominated by fluids and melts derived from subducted sediments. In addition, MORB-like Nb/Ta and Zr/Hf exclude HFSE fractionation by residual HFSE-rich phases in the mantle source of Santorini [*Kirchenbaur and Münker*, 2015]. Thus, the most primitive Santorini samples (<55

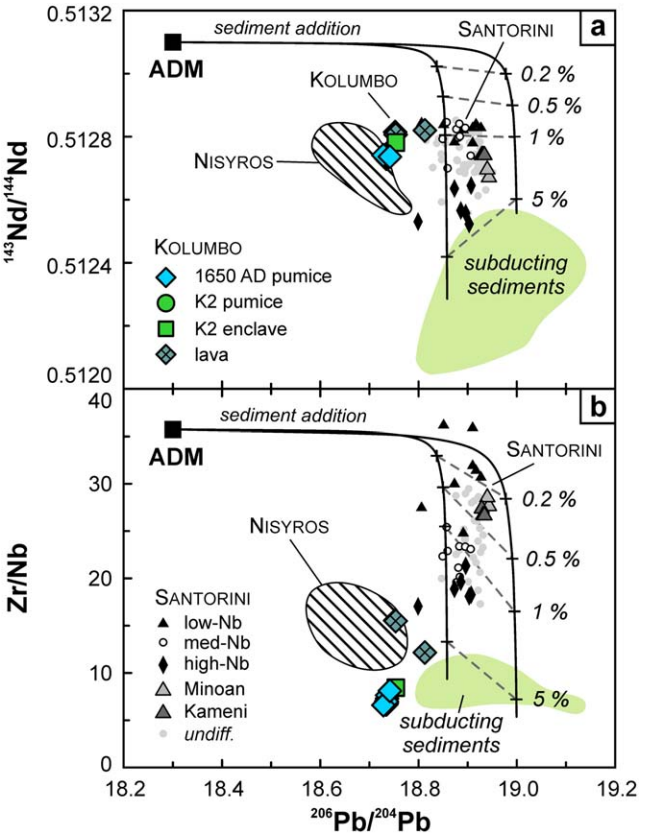

Figure 12. (a) $^{143}Nd/^{144}Nd$ and (b) Zr/Nb versus $^{206}Pb/^{204}Pb$ diagrams showing the variation of Kolumbo, Santorini and Nisyros in combination with the sediment addition model of *Klaver et al*. [2016a]. Addition of subducting Eastern Mediterranean Sea sediments [*Klaver et al*., 2015] to an Aegean depleted mantle (ADM) source successfully explains the Pb-Nd isotope and Zr/Nb variation of Santorini through variable sediment addition, but cannot account for the coupled lower $^{206}Pb/^{204}Pb$ and Zr/Nb of Kolumbo. The similarity of Kolumbo and Nisyros (data from *Buettner et al*. [2005] and *Klaver et al*. [2016a]) suggests that Kolumbo lavas are derived from a mantle source that is more similar to Nisyros than to Santorini, despite the proximity to the latter. See text for further discussion.

wt.% SiO_2) overlap with N-MORB in Nb/Yb and the coupled increase in Nb/Yb and Th content and decrease in $^{143}Nd/^{144}Nd$ from the low-Nb to the high-Nb series (Figure 11) is consistent with sediment addition to an N-MORB mantle source [*Zellmer et al*., 2000; *Bailey et al*., 2009; *Kirchenbaur et al*., 2012; *Kirchenbaur and Münker*, 2015].

The Kolumbo suite has an extrapolated Nb concentration of 5–7 ppm at 53 wt.% SiO_2, which overlaps with the medium-Nb (mean 4.7 ppm Nb) and high-Nb series (mean 7.1 ppm Nb) of *Bailey et al*. [2009]. Nb/Yb also overlaps with the high-Nb series of Santorini, but Th contents are lower and in particular $^{143}Nd/^{144}Nd$ is higher in the primitive Kolumbo samples. This suggests that high Nb/Yb of Kolumbo is not the result of a large subducted sediment contribution as in the high-Nb series of Santorini, but that it more likely reflects a mantle source feature. As Nb/Yb in the Kolumbo suite approaches values for Atlantic E-MORB (Figure 11b), we argue that the higher Nb/Yb points to derivation from a more enriched mantle source compared to Santorini. This is supported by lower Zr/Nb (ca. 12 versus >25; Figure 12) and higher Dy/Yb_N (1.16 versus ~1.0; Figure 9), Nb/Ta (15.5–18 versus 14–16) and Zr/Hf (39–44 versus 35–40) of Kolumbo compared to Santorini. Instead, Kolumbo shares many HFSE and isotope characteristics with Nisyros (Figures 11 and 12), the easternmost active volcanic center of the Aegean arc, ca 150 km to the east.

5.3.2. Pb Isotopes

The most pronounced isotopic difference between Kolumbo and Santorini is found in Pb isotopes. Kolumbo has lower $^{206}Pb/^{204}Pb$ (18.73–18.81) compared to Santorini (18.8–19.0, mostly >18.88) and in particular the recent Kameni dacites and the Minoan Tuff (~18.95; Figure 12). As discussed in section 5.2, Pb isotopes indicate that the distinct crustal differentiation trends of Kolumbo and Santorini are the result of the preferential assimilation of lower- and upper crust, respectively. This difference in assimilants fails to account for the full Pb isotope variability in primitive Kolumbo and Santorini magmas. Here we will test whether this difference can be explained by mantle source heterogeneity as concluded on the basis of the HFSE systematics.

In the case of Santorini, Nd-Pb isotope and trace element systematics can be explained by the addition of 0.5–5% subducting Eastern Mediterranean Sea sediments [*Klaver et al*., 2015] to a depleted N-MORB mantle source [*Bailey et al*., 2009; *Kirchenbaur and Münker*, 2015; *Klaver et al*., 2016a]. Figure 12 shows a mixing model between a depleted mantle source and subducting sediments that is adapted from *Klaver et al*. [2016a]. This model fails to account for the composition of most of the Kolumbo samples as these are displaced to lower $^{143}Nd/^{144}Nd$ compared to the mixing lines. In addition to the HFSE and $^{143}Nd/^{144}Nd$ evidence, another argument against sediment addition is the combination of low Zr/Nb and low $^{206}Pb/^{204}Pb$ in the Kolumbo lavas (Figure 12b). Sediment addition will result in a decrease in Zr/Nb from typical N-MORB values

(~35) [*Sun and McDonough*, 1989] to values typical for continental crust and local subducting sediments (6–11) [*Kirchenbaur and Münker*, 2015; *Klaver et al*., 2015]. Due to the large contrast in Pb contents between depleted mantle and sediment-derived fluids, however, mixing curves are strongly hyperbolic and only a small fraction of sediment is required for the Pb isotopes to be dominated by the composition of the sediment while Zr/Nb is not significantly affected. This is exemplified by the decrease in Zr/Nb at relatively invariable $^{206}Pb/^{204}Pb$ from the low-Nb to the high-Nb group of Santorini (Figure 12b). The coupled low Zr/Nb and low $^{206}Pb/^{204}Pb$ of the Kolumbo lavas is thus incompatible with sediment addition to a mantle source similar to that of Santorini. Hence, the combined HFSE and Nd-Pb isotope evidence requires that the primary melts that are delivered to the crustal magmatic system of Kolumbo are distinct from those of Santorini. Two possible models can account for these variations: i) Kolumbo is derived from the same depleted mantle source as Santorini, but has received a contribution from a low $^{206}Pb/^{204}Pb$, high $^{143}Nd/^{144}Nd$ subducted sediment component that has not been recognized, despite the comprehensive data for subducting sediments in the Eastern Mediterranean that have become available recently [*Kirchenbaur and Münker*, 2015; *Klaver et al*., 2015]; ii) derivation of the Kolumbo magmas from a distinct, more enriched mantle source with, amongst others, high Nb/Yb, low Zr/Nb and low $^{206}Pb/^{204}Pb$. On the basis of the similarity of the primitive Kolumbo samples with Nisyros, the easternmost volcanic center of the Aegean arc, in terms of HFSE systematics and Nd-Pb isotopes, we find most support for the second model. *Klaver et al*. [2016a] related along-arc variations in trace elements and Nd-Pb isotopes between Santorini and Nisyros to heterogeneity of the Aegean mantle wedge that is induced by the infiltration of enriched, subslab mantle through a tear in the African slab underneath western Turkey. A subtle influence of this enriched mantle component can be recognized in some Santorini basalts [*Klaver et al*., 2016a], but the new data suggest that this component is much more pronounced underneath Kolumbo despite the close proximity of the two volcanic centers. Kolumbo is thus geochemically more closely associated with Nisyros, ~150 km to the east, than with its neighbor Santorini. Hence, the main implication of this finding is that pronounced variations in mantle wedge composition can be manifested in arc volcanoes within a single volcanic field. Whereas geochemical variations in primitive arc magmas are commonly attributed to a continental component (either recycled or through crustal assimilation), the role of the mantle wedge is often overlooked. Similar mantle wedge heterogeneity recorded in arc magmas over short (<25 km) distances has also recently been observed in the Southern Volcanic Zone in Chile [*Hickey-Vargas et al*., 2016] and central Italy [*Nikogosian et al*., 2016].

5.4. Petrogenesis of the Kolumbo Suite

The new petrographic and whole rock and mineral geochemical data of the Kolumbo suite can be used to make some inferences on the magmatic system of Kolumbo and the petrogenesis of the rhyolitic pumices. Both the 1650 AD and K2 pumices contain abundant cm-sized mafic inclusions with a texture of acicular amphibole and plagioclase, suggesting that they formed through quenching of hydrous, mafic melts injected into the cooler silicic reservoir. This suggests that mafic injections probably acted as an eruption trigger for both the K2 and 1650 AD eruption [*Sparks et al*., 1977; *Cantner et al*., 2014]. Contacts between the mafic inclusions and the rhyolitic host vary from rounded to angular and chilled margins are poorly developed in the more angular inclusions. The latter likely represent fragments of larger mafic enclaves, possible related to a previous episode of mafic melt injection, which were fragmented and dispersed in the rhyolitic host shortly prior to or during eruption. Small crystal clots consisting of clinopyroxene and plagioclase crystals that are present in the 1650 AD and K2 pumices likely originate in the same way [cf. *Humphreys et al*., 2009; *Braschi et al*., 2014]. The low Cr and Ni contents and andesitic composition of the analyzed mafic inclusion in the K2 pumice indicate that it is not a primitive melt and underwent differentiation and/or significant mixing with the rhyolitic host. Acicular amphibole and plagioclase in the mafic inclusions likely formed as a response to rapid cooling upon injection into the rhyolitic melt. Clinopyroxene macrocrysts in the mafic inclusion and in crystal clots, however, probably represent material that crystallized from the mafic melt at depth prior to its rise to the shallower rhyolitic reservoir. The high Al content of these clinopyroxenes (up to 9 wt.% Al_2O_3; Figure 4) suggests that they crystallized from a melt with a high Al_2O_3 content. Experimental studies have demonstrated that the high H_2O content of arc magmas leads to the suppression of plagioclase crystallization and promotes crystallization of olivine+clinopyroxene±spinel wherlite cumulates at lower crustal pressures, thereby driving the derivative liquid to a high-Al basalt composition [e.g., *Sisson and Grove*, 1993; *Müntener et al*., 2001; *Pichavant and Macdonald*, 2007]. Due to the absence of aluminous fractionating phases, clinopyroxene will become progressively Al-rich with differentiation, resulting in a

negative correlation between Al content and Mg # in cpx (Figure 4). Indeed, such trends are shown by clinopyroxene in arc-root cumulate complexes [e.g., *Jagoutz et al*., 2007]. Hence, we assert that the Al-rich nature of the Kolumbo clinopyroxene macrocrysts attests to a differentiation history in a lower crustal reservoir under hydrous conditions, resulting in the formation of wehrlite cumulates and the generation of high-Al derivative liquids. The andesitic Kolumbo lavas are inferred to have formed through this process as well, given their high Al_2O_3 and Sr contents (Figures 5 and 6).

We argue that the rhyolitic Kolumbo pumices are evolved liquids that formed through differentiation of these high-Al, hydrous arc magmas at depth. *Annen et al*. [2006] have shown that highly evolved, hydrous arc magmas can be generated through prolonged crystal fractionation in a lower crustal reservoir, potentially in combination with mixing with crustal melts. The silicic melts will rise through the crust and stall upon degassing, but can be made eruptible by means of the injection of hot mafic melts. Such a scenario is proposed for the Akrotiri rhyodacites by *Mortazavi and Sparks* [2004], with which the Kolumbo pumices share many geochemical and petrographic characteristics, most notably the presence of amphibole. Residual hornblende in the lower crustal reservoir is capable of imparting the geochemical amphibole signature on the extracted silicic melts [*Davidson et al*., 2007; *Smith*, 2014]. Moreover, assimilation of lower crust during deep differentiation is a plausible means of explaining the characteristic high $^{208}Pb/^{204}Pb$ of the Kolumbo pumices.

Our proposed model of the magmatic system of Kolumbo includes a dominant role for differentiation at the base of the arc crust. Prolonged differentiation and minor hybridization with lower crustal melts produced the Kolumbo rhyolites, which rose near adiabatically and stalled upon degassing to form a partly solidified mush at ca. 5–7 km depth [*Dimitriadis et al*., 2010; *Cantner et al*., 2014]. Evolved, high-aluminium basalts were the parental melts to the Kolumbo lavas, and similar melts were injected in the shallow rhyolitic mush, resulting in the eruption of the inclusion-bearing Kolumbo pumices. Several questions, however, remain unanswered. It is not clear to what extent the model can account for the geochemical similarity of the K2 and 1650 AD pumices, in particular if the suggested ~140 kyr time gap between the two eruptions [*Hübscher et al*., 2015] is correct. Future studies including radiometric dating of the K2 pumice and geochemical data for the units between the K2 and 1650 AD pumices are proposed to further unravel the geochemical and geodynamical evolution of Kolumbo submarine volcano.

6. Conclusions

This study reports the first trace element and Sr-Nd-Hf-Pb isotope data for volcanic products of Kolumbo submarine volcano, situated 15 km to the NE of Santorini. Kolumbo hosts biotite-bearing rhyolitic pumices (~73 wt.% SiO_2, ~4.2 wt.% K_2O) and amphibole-bearing basaltic to andesitic (52–60 wt.% SiO_2) lavas and comagmatic mafic inclusions that were emplaced contemporaneously with the second explosive cycle of Santorini. The rhyolitic pumices display petrographic evidence for differentiation in a lower crustal reservoir in the form of high-Al clinopyroxene relics, before being emplaced in a shallow (5–7 km) magma chamber. As suggested by the presence of quenched mafic enclaves, injection of mafic melts was the likely trigger of the explosive eruptions. A deep differentiation history is corroborated by a signature of high $^{208}Pb/^{206}Pb$ compared to Santorini, which is interpreted to result from preferential assimilation of lower crustal basement. The stability of amphibole at depth has imparted a pronounced geochemical signature on the Kolumbo suite, which is one of the key characteristics of subduction-zone magmatism but conspicuously absent on Santorini. There are marked geochemical differences between Kolumbo and Santorini despite their proximity. In particular, high Nb/Yb (3–4) and low Zr/Nb (12–15), $^{206}Pb/^{204}Pb$ (~18.75) and $^{87}Sr/^{86}Sr$ (~0.7036) at similar $^{143}Nd/^{144}Nd$ (~0.51283) for primitive Kolumbo samples are inconsistent with variable amounts of subducting sediment addition or crustal contamination and likely reflect a source feature. Kolumbo shares this signature with Nisyros, a volcanic center ~150 km to the east that is influenced by the presence of an enriched mantle component in its source. On the basis of the similarity, we propose that the distinct geochemical signature of Kolumbo is imprinted by variations in the mantle wedge underneath the Santorini volcanic field. Thus, despite the close temporal and spatial association of the two volcanic centers, with a distance of only 15 km from crater to crater, we conclude that the Kolumbo suite is distinct from the magmatic products of Santorini in its source and differentiation history. There is no evidence of a recent shallow connection between the two plumbing systems or a genetic link relating the two suites to a common mantle source. The differences between Santorini and Kolumbo emphasize that the geochemical

variation within the Santorini volcanic field is larger than previously assumed. In addition, we recognize that arc volcanoes $\leq$15 km apart can tap unrelated and distinct mantle sources, and that these distinct source signatures can be preserved through highly contrasting crustal evolution pathways.

Acknowledgements
Support for the operation of the E/V *Nautilus* was provided by the US National Oceanic and Atmospheric Administration, Office of Ocean Exploration, and the Ocean Exploration Trust. We thank the captain and crew of the E/V *Nautilus* for their excellent support during the execution of the cruises NA007 and NA014. We would like to acknowledge the help of Bastien Soens with sample preparation and in particular Lisa Hageman for carefully separating enclave fragments from the pumices. The technical staff at VUA, Richard Smeets, Roel van Elsas and Bas van der Wagt, are thanked for their assistance with the analytical work. Sergei Matveev was invaluable for obtaining the EMP data at Utrecht University. Detailed reviews by M. Bizimis, T. Druitt and D. Pyle greatly helped streamline the paper and J. Blichert-Toft is thanked for efficient editorial handling. The MC-ICPMS and TIMS facilities at VUA are funded by the Netherlands Organization for Scientific Research (NWO) through grants 175.107.404.01 and 834.10.001, respectively. The infrastructure used in this study was partly supported by funding from the European Research Council under the European Union's Seventh Framework Program (FP7/2007-2013)/ERC grant agreement 319209; Nexus 1492. The full Kolumbo data set presented in this study is available in the online supporting information (Data Set S1).

References

Aksu, A., G. Jenner, R. Hiscott, and E. İşler (2008), Occurrence, stratigraphy and geochemistry of Late Quaternary tephra layers in the Aegean Sea and the Marmara Sea, *Mar. Geol.*, *252*(3), 174–192.

Alonso-Perez, R., O. Müntener, and P. Ulmer (2009), Igneous garnet and amphibole fractionation in the roots of island arcs: Experimental constraints on andesitic liquids, *Contrib. Mineral. Petrol.*, *157*(4), 541–558.

Andújar, J., B. Scaillet, M. Pichavant, and T. H. Druitt (2015), Differentiation conditions of a basaltic magma from Santorini, and its bearing on the production of andesite in arc settings, *J. Petrol.*, *56*(4), 765–794.

Annen, C., J. Blundy, and R. Sparks (2006), The genesis of intermediate and silicic magmas in deep crustal hot zones, *J. Petrol.*, *47*(3), 505–539.

Arevalo, R., and W. F. McDonough (2010), Chemical variations and regional diversity observed in MORB, *Chem. Geol.*, *271*(1), 70–85.

Bailey, J. C., E. Jensen, A. Hansen, A. Kann, and K. Kann (2009), Formation of heterogeneous magmatic series beneath North Santorini, South Aegean island arc, *Lithos*, *110*(1), 20–36.

Barton, M., and J. P. Huijsmans (1986), Post-caldera dacites from the Santorini volcanic complex, Aegean Sea, Greece: An example of the eruption of lavas of near-constant composition over a 2,200 year period, *Contrib. Mineral. Petrol.*, *94*(4), 472–495.

Bell, K. L., P. Nomikou, S. N. Carey, E. Stathopoulou, P. Polymenakou, A. Godelitsas, C. Roman, and M. Parks (2012), Continued exploration of the Santorini volcanic field and Cretan Basin, Aegean Sea, *Oceanography*, *25*(1), 30–31.

Bezard, R., J. P. Davidson, S. Turner, C. G. Macpherson, J. M. Lindsay, and A. J. Boyce (2014), Assimilation of sediments embedded in the oceanic arc crust: Myth or reality?, *Earth Planet. Sci. Lett.*, *395*, 51–60.

Bohnhoff, M., M. Rische, T. Meier, D. Becker, G. Stavrakakis, and H.-P. Harjes (2006), Microseismic activity in the Hellenic Volcanic Arc, Greece, with emphasis on the seismotectonic setting of the Santorini–Amorgos zone, *Tectonophysics*, *423*(1), 17–33.

Bonneau, M. (1984), Correlation of the Hellenide nappes in the south-east Aegean and their tectonic reconstruction, *Geol. Soc. Spec. Publ.*, *17*(1), 517–527.

Braschi, E., L. Francalanci, S. Tommasini, and G. E. Vougioukalakis (2014), Unraveling the hidden origin and migration of plagioclase phenocrysts by in situ Sr isotopes: The case of final dome activity at Nisyros volcano, Greece, *Contrib. Mineral. Petrol.*, *167*(3), 1–25.

Brenan, J., H. Shaw, F. Ryerson, and D. Phinney (1995), Experimental determination of trace-element partitioning between pargasite and a synthetic hydrous andesitic melt, *Earth Planet. Sci. Lett.*, *135*(1), 1–11.

Buettner, A., I. C. Kleinhanns, D. Rufer, J. C. Hunziker, and I. M. Villa (2005), Magma generation at the easternmost section of the Hellenic arc: Hf, Nd, Pb and Sr isotope geochemistry of Nisyros and Yali volcanoes (Greece), *Lithos*, *83*(1–2), 29–46.

Cadoux, A., B. Scaillet, T. H. Druitt, and E. Deloule (2014), Magma storage conditions of large Plinian eruptions of Santorini volcano (Greece), *J. Petrol.*, *55*(6), 1129–1171.

Cantner, K., S. Carey, and P. Nomikou (2014), Integrated volcanologic and petrologic analysis of the 1650AD eruption of Kolumbo submarine volcano, Greece, *J. Volcanol. Geotherm. Res.*, *269*, 28–43.

Carey, S., K. L. C. Bell, P. Nomikou, G. Vougioukalakis, C. N. Roman, K. Cantner, K. Bejelou, M. Bourbouli, and J. F. Martin (2011), Exploration of the Kolumbo volcanic rift zone, *Oceanography*, *24*(1), 24–25.

Carey, S., P. Nomikou, K. C. Bell, M. Lilley, J. Lupton, C. Roman, E. Stathopoulou, K. Bejelou, and R. Ballard (2013), CO2 degassing from hydrothermal vents at Kolumbo submarine volcano, Greece, and the accumulation of acidic crater water, *Geology*, *41*(9), 1035–1038.

Cottrell, E., J. E. Gardner, and M. J. Rutherford (1999), Petrologic and experimental evidence for the movement and heating of the pre-eruptive Minoan rhyodacite (Santorini, Greece), *Contrib. Mineral. Petrol.*, *135*(4), 315–331.

Davidson, J., S. Turner, H. Handley, C. Macpherson, and A. Dosseto (2007), Amphibole "sponge" in arc crust?, *Geology*, *35*(9), 787–790.

Davidson, J., S. Turner, and T. Plank (2013), Dy/Dy*: Variations arising from mantle sources and petrogenetic processes, *J. Petrol.*, *54*(3), 525–537.

Davidson, J. P. (1987), Crustal contamination versus subduction zone enrichment: Examples from the Lesser Antilles and implications for mantle source compositions of island arc volcanic rocks, *Geochim. Cosmochim. Acta*, *51*(8), 2185–2198.

Dimitriadis, I., C. Papazachos, D. Panagiotopoulos, P. Hatzidimitriou, M. Bohnhoff, M. Rische, and T. Meier (2010), P and S velocity structures of the Santorini–Coloumbo volcanic system (Aegean Sea, Greece) obtained by non-linear inversion of travel times and its tectonic implications, *J. Volcanol. Geotherm. Res.*, *195*(1), 13–30.

Dominey-Howes, D., G. Papadopoulos, and A. Dawson (2000), Geological and historical investigation of the 1650 Mt. Columbo (Thera Island) eruption and tsunami, Aegean Sea, Greece, *Nat. Hazards*, *21*(1), 83–96.

Druitt, T. (2014), New insights into the initiation and venting of the Bronze-Age eruption of Santorini (Greece), from component analysis, *Bull. Volcanol.*, *76*(2), 1–21.

Druitt, T. H., L. Edwards, R. Mellors, D. Pyle, R. Sparks, M. Lanphere, M. Davies, and B. Barreirio (1999), *Santorini Volcano*, The Geological Society, London, U. K.

Elburg, M. A., I. Smet, and E. De Pelsmaeker (2014), Influence of source materials and fractionating assemblage on magmatism along the Aegean Arc, and implications for crustal growth, *Geol. Soc. Spec. Publ.*, *385*(1), 137–160.

Fabbro, G., T. Druitt, and S. Scaillet (2013), Evolution of the crustal magma plumbing system during the build-up to the 22-ka caldera-forming eruption of Santorini (Greece), *Bull. Volcanol.*, *75*(12), 1-22.

Federman, A. N., and S. N. Carey (1980), Electron microprobe correlation of tephra layers from eastern Mediterranean abyssal sediments and the island of Santorini, *Quat. Res.*, *13*(2), 160–171.

Feuillet, N. (2013), The 2011–2012 unrest at Santorini rift: Stress interaction between active faulting and volcanism, *Geophys. Res. Lett.*, *40*, 3532–3537, doi:10.1002/grl.50516.

Fouqué, F.-A. (1879), *Santorin et ses éruptions*, 440 pp., Masson, Paris.

Friedrich, W. L., B. Kromer, M. Friedrich, J. Heinemeier, T. Pfeiffer, and S. Talamo (2006), Santorini eruption radiocarbon dated to 1627-1600 BC, *Science*, *312*(5773), 548-548.

Gertisser, R., K. Preece, and J. Keller (2009), The Plinian lower pumice 2 eruption, Santorini, Greece: Magma evolution and volatile behaviour, *J. Volcanol. Geotherm. Res.*, *186*(3), 387–406.

Griselin, M., J. Van Belle, C. Pomies, P. Vroon, M. Van Soest, and G. Davies (2001), An improved chromatographic separation technique of Nd with application to NdO+ isotope analysis, *Chem. Geol.*, *172*(3), 347–359.

Hickey-Vargas, R., M. Sun, and S. Holbik (2016), Geochemistry of basalts from small eruptive centers near Villarrica stratovolcano, Chile: Evidence for lithospheric mantle components in continental arc magmas, *Geochim. Cosmochim. Acta*. *185*, 358–382.
Hildreth, W., and S. Moorbath (1988), Crustal contributions to arc magmatism in the Andes of central Chile, *Contrib. Mineral. Petrol.*, *98*(4), 455–489.
Hübscher, C., M. Ruhnau, and P. Nomikou (2015), Volcano-tectonic evolution of the polygenetic Kolumbo submarine volcano/Santorini (Aegean Sea), *J. Volcanol. Geotherm. Res.*, *291*, 101–111.
Huijsmans, J. P., M. Barton, and V. J. Salters (1988), Geochemistry and evolution of the calc-alkaline volcanic complex of Santorini, Aegean Sea, Greece, *J. Volcanol. Geotherm. Res.*, *34*(3), 283–306.
Huijsmans, J. P. P. (1985), *Calc-Alkaline Lavas From the Volcanic Complex of Santorini, Aegean Sea, Greece: A Petrological, Geochemical and Stratigraphic Study*, 316 pp., Utrecht Univ., Utrecht, Netherlands.
Humphreys, M. C., T. Christopher, and V. Hards (2009), Microlite transfer by disaggregation of mafic inclusions following magma mixing at Soufrière Hills volcano, Montserrat, *Contrib. Mineral. Petrol.*, *157*(5), 609–624.
Jagoutz, O., O. Müntener, P. Ulmer, T. Pettke, J.-P. Burg, H. Dawood, and S. Hussain (2007), Petrology and mineral chemistry of lower crustal intrusions: The Chilas Complex, Kohistan (NW Pakistan), *J. Petrol.*, *48*(10), 1895–1953.
Keller, J., M. Kraml, and M. Schwarz (2000), Dating major volcanic paroxysms within the deep-sea record: The example of the Thera Formation, Santorini, Greece, in *IAVCEI General Assembly*, 16 pp., Bali, Indonesia.
Kilias, S. P., P. Nomikou, D. Papanikolaou, P. N. Polymenakou, A. Godelitsas, A. Argyraki, S. Carey, P. Gamaletsos, T. J. Mertzimekis, and E. Stathopoulou (2013), New insights into hydrothermal vent processes in the unique shallow-submarine arc-volcano, Kolumbo (Santorini), *Greece, Sci. Rep.*, *3*(2421), 1–13.
Kirchenbaur, M., and C. Münker (2015), The behaviour of the extended HFSE group (Nb, Ta, Zr, Hf, W, Mo) during the petrogenesis of mafic K-rich lavas: The Eastern Mediterranean case, *Geochim. Cosmochim. Acta*, *165*, 178–199.
Kirchenbaur, M., C. Münker, S. Schuth, D. Garbe-Schönberg, and P. Marchev (2012), Tectonomagmatic constraints on the sources of Eastern Mediterranean K-rich lavas, *J. Petrol.*, *53*(1), 27–65.
Klaver, M., T. Djuly, S. de Graaf, A. Sakes, J. Wijbrans, G. Davies, and P. Vroon (2015), Temporal and spatial variations in provenance of Eastern Mediterranean Sea sediments: Implications for Aegean and Aeolian arc volcanism, *Geochim. Cosmochim. Acta*, *153*, 149–168.
Klaver, M., G. R. Davies, and P. Z. Vroon (2016a), Subslab mantle of African provenance infiltrating the Aegean mantle wedge, *Geology*, *44*(5), 367–370.
Klaver, M., R. Smeets, J. M. Koornneef, G. Davies, and P. Vroon (2016b), Pb isotope analysis of ng size samples by TIMS equipped with a 10^{13} Ω resistor using a ^{207}Pb-^{204}Pb double spike, *J. Anal. At. Spectrom.*, *31*, 171–178.
Le Maitre, R. W., P. Bateman, A. Dudek, J. Keller, J. Lameyre, M. Le Bas, P. Sabine, R. Schmid, H. Sorensen, and A. Streckeisen (1989), *A classification of igneous rocks and glossary of terms: Recommendations of the International Union of Geological Sciences Subcommission on the Systematics of Igneous Rocks*, 206 pp., Blackwell Oxford.
Martin, V. M., M. B. Holness, and D. M. Pyle (2006), Textural analysis of magmatic enclaves from the Kameni Islands, Santorini, Greece, *J. Volcanol. Geotherm. Res.*, *154*(1), 89–102.
Mortazavi, M., and R. Sparks (2004), Origin of rhyolite and rhyodacite lavas and associated mafic inclusions of Cape Akrotiri, Santorini: The role of wet basalt in generating calcalkaline silicic magmas, *Contrib. Mineral. Petrol.*, *146*(4), 397–413.
Müntener, O., P. B. Kelemen, and T. L. Grove (2001), The role of H_2O during crystallization of primitive arc magmas under uppermost mantle conditions and genesis of igneous pyroxenites: An experimental study, *Contrib. Mineral. Petrol.*, *141*(6), 643–658.
Newman, A. V., S. Stiros, L. Feng, P. Psimoulis, F. Moschas, V. Saltogianni, Y. Jiang, C. Papazachos, D. Panagiotopoulos, and E. Karagianni (2012), Recent geodetic unrest at Santorini Caldera, Greece, *Geophys. Res. Lett.*, *39*, L06309, doi:10.1029/2012GL051286.
Nikogosian, I., Ö. Ersoy, M. Whitehouse, P. R. D. Mason, J. C. M. de Hoog, R. Wortel, and M. J. van Bergen (2016), Multiple subduction imprints in the mantle below Italy detected in a single lava flow, *Earth Planet. Sci. Lett.*, *449*, 12–19.
Nomikou, P. (2004), Santorini and Nisyros: Similarities and differences between the two calderas of the modern Aegean Volcanic Arc, paper presented at CIESM 2004. Human records of recent geological evolution in the Mediterranean Basin––historical and archaeological evidence, Santorini, Greece.
Nomikou, P., S. Carey, D. Papanikolaou, K. Croff Bell, D. Sakellariou, M. Alexandri, and K. Bejelou (2012), Submarine volcanoes of the Kolumbo volcanic zone NE of Santorini Caldera, Greece, *Global Planet. Change*, *90–91*(0), 135–151.
Nomikou, P., S. Carey, K. L. Croff Bell, D. Papanikolaou, K. Bejelou, M. Alexandri, K. Cantner, and J. F. Martin (2013a), Morphological analysis and related volcanic features of the Kolumbo submarine volcanic chain (NE of Santorini Island, Aegean Volcanic Arc), *Z. Geomorphol.*, *57*(3), 29–47.
Nomikou, P., D. Papanikolaou, M. Alexandri, D. Sakellariou, and G. Rousakis (2013b), Submarine volcanoes along the Aegean volcanic arc, *Tectonophysics*, *597*, 123–146.
Nomikou, P., S. Carey, K. Bell, D. Papanikolaou, K. Bejelou, K. Cantner, D. Sakellariou, and I. Perros (2014a), Tsunami hazard risk of a future volcanic eruption of Kolumbo submarine volcano, NE of Santorini Caldera, Greece, *Nat. Hazards*, *72*(3), 1375–1390.
Nomikou, P., M. Parks, D. Papanikolaou, D. Pyle, T. Mather, S. Carey, A. Watts, M. Paulatto, M. Kalnins, and I. Livanos (2014b), The emergence and growth of a submarine volcano: The Kameni islands, Santorini (Greece), *GeoResJ*, *1*, 8–18.
Oulas, A., et al. (2016), Metagenomic investigation of the geologically unique Hellenic Volcanic Arc reveals a distinctive ecosystem with unexpected physiology, *Environ. Microbiol*, *18*(4), 1122–1136.
Parks, M. M., J. Biggs, P. England, T. A. Mather, P. Nomikou, K. Palamartchouk, X. Papanikolaou, D. Paradissis, B. Parsons, and D. M. Pyle (2012), Evolution of Santorini Volcano dominated by episodic and rapid fluxes of melt from depth, *Nat. Geosci.*, *5*(10), 749–754.
Pe-Piper, G., and D. Piper (2005), The South Aegean active volcanic arc: Relationships between magmatism and tectonics, *Dev. Volcanol.*, *7*, 113–133.
Pichavant, M., and R. Macdonald (2007), Crystallization of primitive basaltic magmas at crustal pressures and genesis of the calc-alkaline igneous suite: Experimental evidence from St Vincent, Lesser Antilles arc, *Contrib. Mineral. Petrol.*, *154*(5), 535–558.
Rizzo, A. L., A. Caracausi, V. Chavagnac, P. Nomikou, P. Polymenakou, M. Mandalakis, G. Kotoulas, A. Magoulas, A. Castillo, and D. Lampridou (2016), Kolumbo submarine volcano (Greece): An active window into Aegean subduction system, *Sci. Rep.*, *6*(28013), 1–9.
Sigurdsson, H., S. Carey, M. Alexandri, G. Vougioukalakis, K. Croff, C. Roman, D. Sakellariou, C. Anagnostou, G. Rousakis, and C. Ioakim (2006), Marine investigations of Greece's Santorini volcanic field, *Eos Trans. AGU*, *87*(34), 337–342, doi:10.1029/2006EO340001.
Sisson, T., and T. Grove (1993), Experimental investigations of the role of H2O in calc-alkaline differentiation and subduction zone magmatism, *Contrib. Mineral. Petrol.*, *113*(2), 143–166.
Smith, D. J. (2014), Clinopyroxene precursors to amphibole sponge in arc crust, *Nat. Commun.*, *5*, 1–6.
Sparks, S. R., H. Sigurdsson, and L. Wilson (1977), Magma mixing: A mechanism for triggering acid explosive eruptions, *Nature*, *267*, 315–318.

Sun, S. s., and W. F. McDonough (1989), Chemical and isotopic systematics of oceanic basalts: Implications for mantle composition and processes, *Geol. Soc. Spec. Publ.*, *42*(1), 313–345.

Thirlwall, M., A. Graham, R. Arculus, R. Harmon, and C. Macpherson (1996), Resolution of the effects of crustal assimilation, sediment subduction, and fluid transport in island arc magmas: Pb-Sr-Nd-O isotope geochemistry of Grenada, Lesser Antilles, *Geochim. Cosmochim. Acta*, *60*(23), 4785–4810.

Thomson, S. N., U. Ring, S. Brichau, J. Glodny, and T. M. Will (2009), Timing and nature of formation of the Ios metamorphic core complex, southern Cyclades, Greece, *Geol. Soc. Spec. Publ.*, *321*(1), 139–167.

Vervoort, J. D., T. Plank, and J. Prytulak (2011), The Hf–Nd isotopic composition of marine sediments, *Geochim. Cosmochim. Acta*, *75*(20), 5903–5926.

Vinci, A. (1985), Distribution and chemical composition of tephra layers from Eastern Mediterranean abyssal sediments, *Mar. Geol.*, *64*(1), 143–155.

Wulf, S., M. Kraml, T. Kuhn, M. Schwarz, M. Inthorn, J. Keller, I. Kuscu, and P. Halbach (2002), Marine tephra from the Cape Riva eruption (22 ka) of Santorini in the Sea of Marmara, *Mar. Geol.*, *183*(1), 131–141.

Zellmer, G., S. Turner, and C. Hawkesworth (2000), Timescales of destructive plate margin magmatism: New insights from Santorini, Aegean volcanic arc, *Earth Planet. Sci. Lett.*, *174*(3), 265–281.